Large-N_c naturalness in coupled-channel meson-meson scattering

T. Ledwig,[1] J. Nieves,[1] A. Pich,[1] E. Ruiz Arriola,[2] and J. Ruiz de Elvira[3]
[1]*Departamento de Física Teórica, IFIC, Universitat de València–CSIC, Apartat Correus 22085, E-46071 València, Spain*
[2]*Departamento de Física Atómica, Molecular y Nuclear and Instituto Carlos I de Fisica Teórica y Computacional, Universidad de Granada, E-18071 Granada, Spain*
[3]*Helmholtz Institute für Strahlen und Kernphysik, Bonn Universität, D-53115 Bonn, Germany*
(Received 15 July 2014; revised manuscript received 27 October 2014; published 16 December 2014)

The analysis of hadronic interactions with effective field theory techniques is complicated by the appearance of a large number of low-energy constants, which are usually fitted to data. On the other hand, the large-N_c limit helps to impose natural short-distance constraints on these low-energy constants, providing a parameter reduction. A Bayesian interpretation of the expected $1/N_c$ accuracy allows for an easy and efficient implementation of these constraints, using an augmented χ^2. We apply this approach to the analysis of meson-meson scattering, in conjunction with chiral perturbation theory to one loop and coupled-channel unitarity, and show that it helps to largely reduce the many existing ambiguities and simultaneously provide an acceptable description of the available phase shifts.

DOI: 10.1103/PhysRevD.90.114020 PACS numbers: 12.39.Fe, 12.38.Gc, 14.20.Dh

I. INTRODUCTION

While the solution of QCD remains a difficult and challenging problem which is being progressively tackled on the lattice, there are two limits where substantial simplifications apply in the continuum: the chiral limit [1] [where the current quark mass m_q is set to zero (see [2,3] for a review)] and the limit of a large number of colors N_c [4,5] (see Ref. [6] for a recent review and references therein), where the strong coupling constant scales as $\alpha_s \sim 1/N_c$. The main common virtue of these simplifications is that at sufficiently low energies, $\sqrt{s} \leq \Lambda$, quark-hadron duality and confinement require that these limits and their corrections can be expressed in purely hadronic terms, with no explicit reference to the underlying quark and gluon degrees of freedom. A well-known example of this duality is given by the Gell-Mann–Oakes–Renner relation, $2m_q|\langle\bar{q}q\rangle| = f_\pi^2 m_\pi^2$, which is $\mathcal{O}(N_c m_\pi^2)$ and relates the current quark mass m_q and the quark condensate $\langle\bar{q}q\rangle$ with the pion decay constant f_π and the pion mass m_π.

Of course, none of these extreme limits is generally expected to faithfully feature the real world. Instead, the *smallness* of the quark mass as compared to $\Lambda_{\rm QCD}$ and the *largeness* of $N_c = 3$ as compared to unity suggest a sensible hierarchy where an expansion in the u, d, s quark masses and a $1/N_c$ expansion may be combined in a suitable way to attempt a credible description of hadron properties and their interactions. Within an effective Lagrangian approach [7], and using the low-energy degrees of freedom (Goldstone bosons) of the nonlinear sigma model [8], a chiral perturbation theory (χPT) to one loop was thus designed [9,10]. On the other hand, the leading tree-level structure implied by the large-N_c limit suggests using a resonance chiral theory (RχT) to successfully saturate the low-energy properties [11–13]. It has been shown that resonance saturation arises quite naturally [14] from the short-distance constraints on the effective hadronic theory stemming from the underlying high-energy behavior of QCD for spacelike momenta.

This scheme is implemented in terms of chiral effective Lagrangians displaying explicitly the relevant hadronic degrees of freedom, characterized by (i) a *finite* number of fields representing stable particles, in the large-N_c limit, with masses $M_R = \mathcal{O}(N_c^0) \lesssim \Lambda$, (ii) $\mathcal{O}(m_q)$ suppressed couplings to pseudoscalar mesons, and (iii) n-mesonic $\mathcal{O}(N_c^{1-n/2})$ suppressed couplings. The decay rates of these states are suppressed, $\Gamma_R = \mathcal{O}(N_c^{-1})$, and are thus resonances. The calculation of quantum corrections, besides restoring unitarity perturbatively within the relevant Λ-truncated Hilbert space, accounts for the scale dependence of the couplings in the Lagrangian, as they effectively and implicitly incorporate the degrees of freedom which have been integrated out. The number of low-energy couplings (LECs) depends on how many independent terms can be written in the effective Lagrangian with fields and their derivatives, so that they naturally scale with inverse powers of the breakdown scale Λ. As it is well known, this number grows rapidly with the order of the expansion, and predictive power relies heavily on having more data than couplings. Large-N_c arguments have helped in fixing the bulk of the scale-independent contribution for the LECs at $\mathcal{O}(p^4)$ and $\mathcal{O}(p^6)$ [see, however, [15] for an exception at $\mathcal{O}(p^6)$].

In this paper we are concerned with the implications of next-to-leading order (NLO) χPT and leading order (LO) $1/N_c$ corrections in the description of the interactions among pseudoscalar mesons belonging to the flavor octet

and below a given energy cutoff, which will be set at $\sqrt{s_{\max}} \sim 1.1$–1.2 GeV $\equiv \Lambda_R$ for definiteness. This energy cutoff provides a motivation to truncate the infinite tower of meson states to just one per quantum number (except for the 0^{++} scalar and 0^{-+} pseudoscalar multiplets, where independent octet and singlet states are considered). At first order in the $1/N_c$ expansion, terms with more than one trace and loops are suppressed; therefore, we only include tree-level resonance contributions. Moreover, we neglect interactions between different resonance channels which, although allowed by the theory symmetries, are not needed in this work.

Furthermore, as argued in Ref. [16], in addition to the tree-level meson-exchange diagrams, one should also foresee contact pieces, which depend on the high-energy cutoff Λ_R. In that work, $\Lambda_R \sim 700$ MeV and thus only elastic $\pi\pi$ scattering was possible. On the other hand, when $\Lambda_R \sim 1.2$ GeV all pseudoscalar-pseudoscalar channels are open; thus, coupled-channel unitarity plays a decisive role. We use here the Bethe-Salpeter equation (BSE) approach, within the on-shell renormalization scheme [17] conveniently extended to the coupled-channel case, which restores exact two-body unitarity, thereby enlarging the scope of the previous work [16] to include coupled channels. This BSE on-shell scheme is characterized by the appearance of nonperturbative subtraction constants, C_{IJ}, and a perturbative matching procedure to reproduce LO $1/N_c$ and NLO χPT. In all, we need 24 independent parameters which must be fixed from fitting scattering data or pseudodata, a rather impractical situation. We will show how a judicious fitting strategy, based on the natural expectation that NLO $1/N_c$ corrections are at the $\sim$30% level, provides good fits with reasonable parameters.

Before embarking on a more involved discussion, let us explain the main idea behind the present work. In the chiral limit, $m_\pi \to 0$, QCD has only one dimensionful parameter which can be chosen to be the pion weak decay constant, f. In the large-N_c limit $f = \mathcal{O}(\sqrt{N_c})$, and hence meson masses must scale as $M_R \sim f/\sqrt{N_c}$ and meson couplings as $G_R \sim f$. That means that we expect an expansion of the form

$$\frac{\sqrt{N_c} M_R}{f} = a_R \left[1 + \frac{\xi_R}{N_c} + \cdots \right] \tag{1}$$

where a_R and ξ_R are numerical dimensionless coefficients of order one. The basic idea to be explored in the present work is the use of this information when we have a good estimate for the LO a_R, but no information on the NLO term ξ_R. Under these circumstances, we may *assume* that ξ_R is a random variable normally distributed, $\langle \xi_R \rangle = 0$ and $\langle \xi_R^2 \rangle = \mathcal{O}(1)$, in which case the variable (for simplicity, couplings G_R are omitted)

$$\chi^2_{\rm th} = \sum_R \xi_R^2, \qquad \xi_R = \frac{\sqrt{N_c} M_R/a_R - f}{f/N_c} \tag{2}$$

follows a χ^2 distribution if the different ξ_R's are uncorrelated, $\langle \xi_R \xi_{R'} \rangle = \delta_{R,R'} \langle \xi_R^2 \rangle$. In the absence of further information, χ^2 is minimized by our guess of the parameters M_R and G_R. However, if we have further data which can be described theoretically by these parameters, M_R, G_R, we may refine our initial guess by adding to Eq. (2) the standard χ^2 term used to carry out a fit to these data. In the first part of the paper we analyze how the LO coefficients can be estimated. In the second part we show how to profit from these estimates in meson-meson scattering.

The paper is organized as follows. In Sec. II we discuss and motivate short-distance constraints in the large-N_c limit and their consequences in the light of data and lattice studies. In Sec. III we analyze how the naturalness of leading-$1/N_c$ corrections provides a sensible estimate on the expected uncertainties of low-energy constants. The formalism for coupled-channel unitarized meson-meson scattering and some specific features are reviewed in Sec. IV. Our fitting strategies and main numerical results are presented in Sec. V. Finally, in Sec. VI we summarize our points and come to the conclusions.

II. LARGE-N_c SHORT-DISTANCE CONSTRAINTS

A. Motivation

In this section we analyze some important conditions which arise from imposing the best possible high-energy behavior of field correlators in a low-energy truncated hadronic theory, compatible with the known behavior in QCD. This leads to a sensible parameter reduction, based on estimates of a_R in Eq. (1), which will be very helpful in our analysis of meson-meson scattering. These short-distance constraints are obtained within a large-N_c framework and when the low-energy theory is limited to spin 0 and 1 resonances, and they allow for a complete parameter reduction in the chiral limit; all couplings and masses can be explicitly expressed in terms of the pion weak decay constant and the number of colors N_c. In order to appreciate the result, it is important to spell out which are the main assumptions and approximations leading to it.

As already mentioned, in the large-N_c limit, interactions among hadrons and with external currents are suppressed. This allows us to set up a hierarchy in terms of an infinite number of quantum hadronic fields $R_i(x)$ and their derivatives, compatible with the symmetries at all energies, which can be written at tree level in terms of a real local Lagrangian with a given set of coupling constants G_{R_i} and hadron masses M_{R_i}. Unitarity is recovered perturbatively by computing quantum corrections in a loop expansion. As we are interested in an intermediate-energy description, say $\sqrt{s} \leq \Lambda_R$, we need only consider explicitly a finite number of fields which are active below this cutoff scale, $M_{R_i} \lesssim \Lambda_R$.

Heavier states, $\Lambda_R \lesssim M_{R_i}$, are included implicitly through the couplings $G_{R_i}(\Lambda, M_{R_i})$ and masses $M_{R_i}(\Lambda, M_{R_i})$ appearing in the low-energy Lagrangian. In our case we will take $\Lambda_R \sim 1.1$ GeV. This means, in practice, taking, besides the pion, explicit $S(0^{++})$, $P(0^{-+})$, $V(1^{--})$ and $A(1^{++})$ fields whose masses are smaller than the cutoff, m_V, m_S, m_P, $m_A \lesssim \Lambda_R$.

B. Resonance Lagrangian

The RχT Lagrangian describes the dynamics of Goldstone and massive meson multiplets of the type $S(0^{++})$, $P(0^{-+})$, $V(1^{--})$ and $A(1^{++})$ [11–13], in terms of a set of masses $m_\pi, m_S, m_P, m_V, m_A$ and couplings $F_A, F_V, G_V, c_d, c_m, d_m, \tilde{c}_d, \tilde{c}_m, \tilde{d}_m, f_\pi$, which can be determined phenomenologically. We will only need the lowest-order couplings:

$$\begin{aligned}\mathcal{L}_2 = {} & \frac{f^2}{4}\langle D_\mu U^\dagger D^\mu U + U^\dagger\chi + \chi^\dagger U\rangle \\ & + \sum_i \left\{ \frac{F_{V_i}}{2\sqrt{2}}\langle V_i^{\mu\nu} f_{+\mu\nu}\rangle + \frac{iG_{V_i}}{\sqrt{2}}\langle V_i^{\mu\nu}[u_\mu, u_\nu]\rangle \right\} \\ & + \sum_i \frac{F_{A_i}}{2\sqrt{2}}\langle A_i^{\mu\nu} f_{-\mu\nu}\rangle + \sum_i id_{m_i}\langle P_i \chi_-\rangle \\ & + \sum_i \{c_{d_i}\langle S_i u^\mu u_\mu\rangle + c_{m_i}\langle S_i \chi_+\rangle\}. \end{aligned} \tag{3}$$

The matrix $U(\phi) = u(\phi)^2 = \exp\{i\sqrt{2}\Phi/f\}$ contains the Goldstone fields, $\chi = 2B_0\mathcal{M}$ is the explicit breaking of chiral symmetry through the quark mass matrix $\mathcal{M}$, $u_\mu \equiv iu^\dagger D_\mu U u^\dagger$, $f_\pm^{\mu\nu} \equiv uF_L^{\mu\nu}u^\dagger \pm u^\dagger F_R^{\mu\nu}u$, $\chi_\pm \equiv u^\dagger\chi u^\dagger \pm u\chi^\dagger u$, and $\langle\rangle$ denotes a three-dimensional flavor trace. We refer to Refs. [11–13] for notations and technical details.

Clearly, in the chiral limit all dimensionful quantities should scale with $\Lambda_{\rm QCD}$ or, alternatively, with $f \approx f_\pi \sim \Lambda_{\rm QCD}$. As we now discuss, it is remarkable that a combination of the large-N_c limit with a set of short-distance constraints, based on imposing asymptotic QCD conditions stemming from the operator product expansion (OPE), and with a minimal hadronic ansatz, yields quite naturally to this scaling behavior.

C. Short-distance constraints at leading order

Two-, three- and four-point-function constraints have been discussed in Ref. [14] for SS, VV, AA, PP, VPP and SPP correlators. They determine the RχT couplings in terms of the pion decay constant. For illustration purposes, we review here some of the short-distance constraints discussed in [14]. At leading order in $1/N_c$, the two-Goldstone matrix element of the vector current and the matrix element of the axial current between one Goldstone and one photon are characterized, respectively, by the vector and axial-vector form factors:

$$\begin{aligned} F_V(t) &= 1 + \sum_i \frac{F_{V_i}G_{V_i}}{f_\pi^2}\frac{t}{m_{V_i}^2 - t}, \\ G_A(t) &= \sum_i \frac{2F_{V_i}G_{V_i} - F_{V_i}^2}{m_{V_i}^2} + \frac{F_{A_i}^2}{m_{A_i}^2 - t}. \end{aligned} \tag{4}$$

Since they should vanish at $t \to \infty$, the resonance couplings should satisfy

$$\sum_i F_{V_i}G_{V_i} = f_\pi^2, \qquad \sum_i \frac{2F_{V_i}G_{V_i} - F_{V_i}^2}{m_{V_i}^2} = 0. \tag{5}$$

In the same way, the leading-$1/N_c$ contribution to the πK scalar form factor is given by

$$F_{K\pi}^S(t) = 1 + \sum_i \frac{4c_{m_i}}{f_\pi^2}\left[c_{d_i} + (c_{m_i} - c_{d_i})\frac{m_K^2 - m_\pi^2}{m_{S_i}^2}\right]\frac{t}{m_{S_i}^2 - t}. \tag{6}$$

Imposing again that $F_{K\pi}^S(t)$ should vanish when $t \to \infty$, we get

$$4\sum_i c_{d_i}c_{m_i} = f_\pi^2, \qquad \sum_i \frac{c_{m_i}}{m_{S_i}^2}(c_{m_i} - c_{d_i}) = 0. \tag{7}$$

Further constraints arising from the Weinberg and $SS - PP$ sum rules are also discussed in [14]. All these large-N_c constraints involve an infinite tower of resonances.

D. Results with single-resonance saturation

Assuming an exact U(3) symmetry and that, at low energies, each infinite resonance sum is dominated by the first meson nonet with the corresponding quantum numbers, the short-distance constraints determine the RχT couplings [14],

$$\begin{aligned} f_\pi = F_A = F_V/\sqrt{2} &= \sqrt{2}G_V = 2c_d = 2c_m = 2\sqrt{2}d_m \\ &= 2\sqrt{3}\tilde{c}_d = 2\sqrt{3}\tilde{c}_m = 2\sqrt{6}\tilde{d}_m, \end{aligned} \tag{8}$$

and give the mass relations $m_A = \sqrt{2}m_V$ and $m_P = \sqrt{2}m_S$. Imposing, in addition, a proper short-distance behavior for the elastic $\pi\pi$ scattering amplitude, it was found in Ref. [16] that, in the absence of tensor couplings, $m_S = m_V$. The absolute mass scale can be further related to f_π by requiring the PVV form factor to fall at large momentum as predicted by QCD [18]. One finds[1]

[1]The same relation between m_V and f_π was obtained by identifying the quark-model one-loop pion radius [19] with vector-meson dominance [20]. This is equivalent to identifying the resonance-saturation prediction for the χPT LECs with the results obtained in the chiral quark model [2,21]. Invoking quark-hadron duality, one also obtains the relations for the other masses within the spectral quark model [22,23].

$$m_S = m_V = \frac{m_P}{\sqrt{2}} = \frac{m_A}{\sqrt{2}} = \pi\sqrt{\frac{24}{N_c}} f_\pi. \tag{9}$$

The first relation complies with $m_S - m_V = \mathcal{O}(N_c^{-1}) + \mathcal{O}(m_\pi N_c^0)$, discussed in Ref. [24] and obtained after identifying m_V and m_ρ in the large-N_c limit. This amounts, in particular, also to the width/mass ratios[2]

$$\frac{\Gamma_V}{m_V} = \frac{\pi}{4N_c}[1 + \mathcal{O}(N_c^{-1})],$$
$$\frac{\Gamma_S}{m_S} = \frac{9\pi}{8N_c}[1 + \mathcal{O}(N_c^{-1})], \tag{10}$$

which compare rather well with the experimental Breit-Wigner values for Γ_ρ/m_ρ and Γ_σ/m_σ [16]. As noted in [25], the locations of the Breit-Wigner and pole masses differ by $\mathcal{O}(N_c^{-2})$ corrections.

Although consistent with the large-N_c counting, these relations assume that the high-energy properties can be properly saturated with a minimal set of resonances. Therefore, they are subject to corrections already at LO in $1/N_c$, due to the neglected higher-energy states. These corrections are difficult to estimate when there are more massive states than constraints. Actually, in the opposite case, and for the single-resonance case, there may appear contradicting constraints [26] (see the comprehensive discussion in Ref. [27]) which provide similar relations with *different* and N_c-independent numerical factors. There is of course the pertinent question on *what* numerical values should be used in the Λ_R-truncated RχT effective Lagrangian, since it is itself of LO in the $1/N_c$ expansion.

We note in this regard that resonances manifest as poles of scattering amplitudes in the second Riemann sheet (SRS), $\sqrt{s_R} = m_R - i\Gamma_R/2$, and, in principle, have vanishing widths in the large-N_c limit.[3] The NLO corrections are $\mathcal{O}(N_c^{-1})$, corresponding to a mass shift Δm_R and the width Γ_R which are numerically alike [18]. Ultimately, QCD determines the proper numerical factors.

E. Comparison with large-N_c lattice calculations

The large-N_c limit has recently been implemented on the lattice by numerically changing $N_c = 2, 3, 4, 5, 6, 7\ldots$ [34,35] and extracting meson masses and decay widths in the quenched approximation, since corrections are $1/N_c^2$ suppressed (the fermion determinant providing the LO corrections in $1/N_c$ was not included). Other studies find $m_\rho/f_\pi = [7.08(10), 7.21(10)]$, $m_{a_1}/f_\pi = [13.16(21), 13.26(21)]$, $m_{\pi^*}/f_\pi = [15.61(34), 15.70(34)]$ and $f_\rho/f_\pi = [1.861(30), 1.875(31)]$ for $m_q = [0, m_{ud}]$, respectively, to be compared with Eq. (9) where one has $m_V/f_\pi = 8.89$, $m_A/f_\pi = 12.57$, $m_P/f_\pi = 12.57$ and $f_V/f_\pi = 1.41$ (note a $\sqrt{2}$ factor of difference between the normalization for f_V used here and that of Ref. [34]; regarding the decay constants, due to the lack of nonperturbative renormalization at $N_c = \infty$, an error of 8% should be associated with the values quoted above and taken from Table 4 of Ref. [34]). Unfortunately, no predictions have been made yet for the troublesome 0^{++} scalar mesons on the lattice at large N_c. Nonetheless, the comparison is good enough to discard a purely accidental agreement with Eqs. (8) and (9), not only at the phenomenological level, but also in the large-N_c limit of QCD.

On dimensional grounds the parameter reduction in QCD, in the chiral limit, is obvious from a large-N_c counting point of view and the existence of a unique dimensionful scale f_π. One could, of course, take these exact lattice values as an initial guess for our analysis below; they are subjected to $\mathcal{O}(1/N_c)$ and chiral corrections. Unlike our estimates, they get no corrections from higher-energy states. Unfortunately, some of the needed parameters are still missing, so we will content ourselves with our estimates for couplings and mass relations, Eqs. (8) and (9), respectively, based on just one single resonance saturation.

III. NATURAL SIZE OF $1/N_c$ CORRECTIONS

The structure of the chiral expansion in powers of $m_\pi^2/(4\pi f_\pi)^2$ (up to chiral logarithms $\sim \log m_\pi^2$) is well understood and has been worked out in much detail for many processes. Actually, the chiral-loop $\mathcal{O}(p^n)$ corrections are themselves of $\mathcal{O}(N_c^{-n/2})$. However, much less is known about what are the expected and genuine corrections within a $1/N_c$ expansion. While at LO only tree-level diagrams contribute, with the exchange of an infinite number of meson resonances, quantum loops with massive states propagating in the internal lines need to be considered at the NLO. Subleading-$1/N_c$ quantum corrections involving a limited number of resonances have already been investigated [36–42]. A simple rule of thumb is that they are naturally expected to have a 30% accuracy. One vivid demonstration of this naive expectation is given by the width/mass ratio for meson and baryon resonances which scales as $\Gamma/M \leq \mathcal{O}(N_c^{-1})$ [4,5], suggesting a relative 30% ratio, whereas the PDG [43] (spin-weighted) average values *both* for mesons and baryons containing u, d, s flavors are identical and equal to $\langle \Gamma/M \rangle = 0.12(8)$ [44,45],

[2]The first relation is a direct consequence of the discussion in Sec. V of Ref. [24] and Eq. (9), while the scalar one is deduced from the constraint $\Gamma_S/m_S = 9\Gamma_V/2m_V$ rederived, for instance, in Ref. [16] in the absence of tensor couplings from the Adler and σ sum rules within the single-resonance approximation scheme.

[3]Even though behaviors of the poles with nonvanishing widths in the large-N_c limit have been described in the literature [16,28–32], it has been recently reviewed in [33] that it is not possible to find any meson configurations in terms of quarks and gluons with nonvanishing widths in the large-N_c limit coupled to meson-meson channels.

where the uncertainty itself is compatible with a subleading-$1/N_c$ correction.

In order to motivate our approach to meson-meson scattering below, we illustrate the size of $1/N_c$ corrections for the LECs $L_{1,\ldots,10}$. As already noted, RχT predicts their leading-N_c value [11,12], but quite remarkably, no errors on that estimate are ever quoted (besides the scale dependence which is $1/N_c$ suppressed and is usually taken to be $\mu = m_\rho$).

Using Eqs. (8) and (9) (see [14]), one obtains the following set of relations among the LECs[4]:

$$2L_1 = L_2 = -\frac{L_3}{2} = \frac{L_5}{2} = \frac{L_8}{3} = \frac{L_9}{4} = -\frac{L_{10}}{3} = \frac{N_c}{192\pi^2},$$
$$L_4 = L_6 = L_7 = 0, \tag{11}$$

which are valid up to corrections of $\mathcal{O}(N_c^0)$. A rule-of-thumb estimate for the size of the subleading corrections is $\Delta L_i = L_i/N_c$. The situation is illustrated in Table I where we give the phenomenological values of the LECs from $\mathcal{O}(p^4)$ and $\mathcal{O}(p^6)$ fits, compiled in Ref. [47].[5] The column labeled "RχT" shows the resonance-exchange predictions, using input values for m_V and m_S [11,12,14]. Finally, the third column collects the estimations stemming from the short-distance constraints of Eq. (11), with an error L_i/N_c. The agreement with the $\mathcal{O}(p^4)$ phenomenological LECs is somehow deteriorated at $\mathcal{O}(p^6)$, when NNLO chiral corrections are taken into account in the fits. The χPT-loop contributions included at NLO and NNLO are themselves of $\mathcal{O}(N_c^{-1})$ and $\mathcal{O}(N_c^{-2})$, respectively, but the RχT predictions refer to the large-N_c limit and, therefore, are subject to $1/N_c$ corrections. Once our rule-of-thumb expected error of about 33% is considered, the fitted values of the LECs are consistent with the large-N_c estimates. The differences in the values obtained when alternative short-distance constraints are invoked are also comparable [27]. The upshot of the previous discussion is that we naturally expect the $1/N_c$ corrections to the RχT parameters p_i to be of the form

$$p_i = p_i^{\text{Large}-N_c}\left(1 + \frac{\xi_i}{N_c}\right), \tag{12}$$

where ξ_i is of order unity and could, in principle, be calculated. However, if no complete information is available, we may, for the time being, *assume* that ξ_i is a random variable, with $\langle \xi_i \rangle = 0$ and $\langle \xi_i \xi_j \rangle = \delta_{ij}\langle \xi_i^2 \rangle$. Of course, one can improve the bias $\langle \xi_i \rangle = 0$ by adding chiral corrections explicitly. The important feature is that this naturalness assumption will impose rough but *a priori* expectations on the values of the LECs. If ξ_i are Gaussian parameters, then

$$\chi^2_{\text{th}} = \sum_{i=1}^{N} \xi_i^2 = \sum_{i=1}^{N} \left(\frac{p_i - p_i^{\text{Large}-N_c}}{p_i^{\text{Large}-N_c}/N_c}\right)^2 \tag{13}$$

follows a χ^2 distribution. This point of view will be very helpful below when we analyze coupled-channel meson-meson scattering in the pseudoscalar sector.

TABLE I. Predicted values of the χPT LECs (in units of 10^{-3}) obtained from RχT [11,12], i.e. the leading-$1/N_c$ single-resonance approximation, and from the short-distance constraints of Eq. (11), compared with $\mathcal{O}(p^4)$ and $\mathcal{O}(p^6)$ phenomenological determinations at $\mu = m_\rho$ [47].

Parameter	RχT	Eq. (11)	$\mathcal{O}(p^4)$	$\mathcal{O}(p^6)$
L_1	0.90	0.75(25)	0.70(30)	0.43(12)
L_2	1.80	1.5(5)	1.3(7)	0.73(12)
L_3	−4.30	−3.0(1.0)	−4.4(2.5)	−2.35(37)
L_4	0.00	0.0(3)	−0.3(5)	∼0.20
L_5	2.10	3.0(1.0)	1.4(5)	0.97(11)
L_6	0.00	0.0(3)	−0.2(3)	∼0.00
L_7	−0.30	0.0(3)	−0.4(2)	−0.31(14)
L_8	0.80	1.2(4)	0.9(3)	0.60(18)
L_9	7.10	6.0(2.0)	6.9(7)	5.93(43)
L_{10}	−5.40	−4.50(1.5)	−5.5(7)	−5.09(47)

IV. PION-PION AND PION-KAON SCATTERING

We will analyze experimental or phenomenological data for the $\pi\pi$ and $K\pi$ scattering processes:

$$\pi\pi \to \pi\pi, \qquad \pi\pi \to K\bar{K}, \qquad K\pi \to K\pi. \tag{14}$$

The two-body kinematics (Fig. 1) is parametrized by the Mandelstam variables $s = (k_1 + k_2)^2$, $t = (k_1 - k_3)^2$ and $u = (k_1 - k_4)^2$, with $\sqrt{s}$ the total energy in the center-of-mass (CM) system. In our case here, we consider a CM

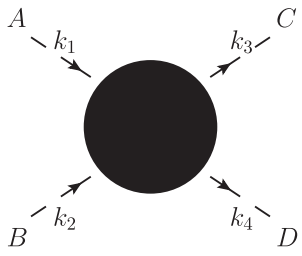

FIG. 1. Meson-meson scattering process $A + B \to C + D$, with incoming momenta k_1, k_2 and outgoing momenta k_3, k_4. Dashed lines denote pseudoscalar mesons and the black dot their interaction.

[4]When the η_1 is integrated out, L_7 receives a contribution proportional to $1/M_{\eta_1}^2 \sim \mathcal{O}(N_c^2)$ [10]. However, the large-N_c counting is no longer consistent if one takes the limit of a heavy η_1 mass (N_c small) while keeping m_s small [46].

[5]The recent global fits of Refs. [48,49] list many results for $L_{1,\ldots,8}(m_\rho)$. See also the recent NLO determinations: $L_9(m_\rho) = 7.9(4) \times 10^{-3}$ [41], $L_{10}(m_\rho) = -4.06(39) \times 10^{-3}$ [50] and $L_{10}(m_\rho) = -3.46(32) \times 10^{-3}$ [51].

energy ranging from $\sqrt{s} = 280$ MeV up to ≈1200 MeV. At these energies the following additional channels are open:

$$\pi\pi \to \eta\eta, \qquad K\bar{K} \to \eta\eta, \qquad K\bar{K} \to K\bar{K},$$
$$\eta\eta \to \eta\eta, \qquad K\eta \to K\pi. \tag{15}$$

Since in all processes the isospin and strangeness is conserved, one can write each scattering amplitude in terms of its contributions of total isospin I, with $I = 0, \frac{1}{2}, 1, \frac{3}{2}, 2$ the only possible values here, and strangeness. Choosing s and the scattering angle θ as the independent variables, each isospin-projected amplitude $T_I(s)$ can be further decomposed into its individual contributions with total angular momentum J (for the sake of brevity, we will not make explicit reference to the strangeness quantum number):

$$T_I(s,t,u) = \sum_{J=0}^{\infty} (2J+1) T_{IJ}(s) P_J(\cos\theta), \tag{16}$$

$$T_{IJ}(s) = \frac{1}{2N}\int_{-1}^{+1} d(\cos\theta) P_J(\cos\theta) T_I(s,t,u) = -16\pi \frac{1}{2i\rho(s)}[\eta_{IJ}(s) e^{2i\delta_{IJ}(s)} - 1], \tag{17}$$

with $P_J(x)$ the Legendre polynomials and $\rho(s)$ a channel-dependent kinematical factor defined below. N is a normalization factor to account for identical particles, such that $N = 2$ if all the particles in the process are identical and $N = 1$ otherwise. Since we are working in the isospin limit, we consider the three pions to be identical. Therefore, in our case, $N = 2$ only for $\pi\pi \to \pi\pi$ and $\eta\eta \to \eta\eta$ processes. Explicitly, we analyze data for the three channels in Eq. (14) that come in terms of the scattering amplitudes $T_{IJ}(s)$, phase shifts $\delta_{IJ}(s)$ and inelasticities $\eta_{IJ}(s)$, defined in Eq. (17). To address the resonance properties, a unitarized framework is needed which leads to the inclusion of coupled channels at higher energies. Because of this, we need, in addition to the above three channels, a theoretical description of the ones in Eq. (15). In that sense, the present work is an extension of Ref. [16] to more channels and higher scattering energies.

Meson-meson scattering within one-loop χPT was analyzed by Gómez-Nicola and Peláez in Ref. [52] where, in addition, unitarization was implemented via the inverse amplitude method (IAM). A naive addition of the missing LO contributions in $1/N_c$, within this scheme, would violate either unitarity or analyticity.[6] We use here a scheme based on the Bethe-Salpeter equation (BSE) to restore two-body unitarity. The BSE on-shell scheme for the non-coupled channel was already described in Refs. [17,53] for χPT and used in [16] when LO $1/N_c$ corrections were further included. The generalization to the coupled-channel situation needed here is straightforward. Let us consider the matrix $T_{IJ}(s)$ incorporating the partial-wave amplitudes of all relevant processes $AB \to CD$:

$$T_{IJ}(s) = \begin{bmatrix} T_{IJ}^{\pi\pi\to\pi\pi}(s) & T_{IJ}^{\pi\pi\to K\bar{K}}(s) & T_{IJ}^{\pi\pi\to\eta\eta}(s) \\ T_{IJ}^{K\bar{K}\to\pi\pi}(s) & T_{IJ}^{K\bar{K}\to K\bar{K}}(s) & T_{IJ}^{K\bar{K}\to\eta\eta}(s) \\ T_{IJ}^{\eta\eta\to\pi\pi}(s) & T_{IJ}^{\eta\eta\to K\bar{K}}(s) & T_{IJ}^{\eta\eta\to\eta\eta}(s) \end{bmatrix}, \tag{18}$$

for channels $\pi\pi \to \pi\pi$ and $\pi\pi \to K\bar{K}$, and

$$T_{IJ}(s) = \begin{bmatrix} T_{IJ}^{K\pi\to K\pi}(s) & T_{IJ}^{K\pi\to K\eta}(s) \\ T_{IJ}^{K\eta\to K\pi}(s) & T_{IJ}^{K\eta\to K\eta}(s) \end{bmatrix}, \tag{19}$$

for channel $K\pi \to K\pi$. All $T_{IJ}^{AB\to CD}(s)$ are defined through Eq. (17), and the explicit form of the amplitudes $T_I(s,t,u)^{AB\to CD}$ is given in Appendix A. Note that some of the above matrix elements are trivially zero from isospin or angular momentum conservation. For instance, in the $I = 2$, $J = 0$ channel, only $T_{IJ}^{\pi\pi\to\pi\pi}(s)$ is different from zero.

Coupled-channel unitarity is most simply expressed in terms of the inverse matrix $T_{IJ}^{-1}(s)$ as

$$\mathrm{Im} T_{IJ}^{-1}(s) = -\mathrm{Im}\bar{\mathcal{I}}_0(s), \tag{20}$$

where $\bar{\mathcal{I}}_0$ is a diagonal matrix of one-loop integrals characterizing the elastic two-body rescattering:

$$\bar{\mathcal{I}}_0(s) = \mathrm{diag}[\bar{I}_0^{\pi\pi}(s), \bar{I}_0^{K\bar{K}}(s), \bar{I}_0^{\eta\eta}(s)] \tag{21}$$

or

$$\bar{\mathcal{I}}_0(s) = \mathrm{diag}[\bar{I}_0^{K\pi}(s), \bar{I}_0^{K\eta}(s)] \tag{22}$$

for the $\pi\pi$ and $K\pi$ cases, respectively. With two identical mesons,

$$\bar{\mathcal{I}}_0^{\phi\phi}(s) = \frac{1}{16\pi^2}\rho_\phi(s) \ln\left[\frac{\rho_\phi(s)+1}{\rho_\phi(s)-1}\right], \tag{23}$$

where $\rho_\phi(s) = \sqrt{1 - 4m_\phi^2/s}$ and

$$\mathrm{Im}\bar{\mathcal{I}}_0^{\phi\phi}(s) = -\theta(s - 4m_\phi^2)\frac{1}{16\pi}\rho_\phi(s). \tag{24}$$

The general expression in the case of two different mesons can be found in Eq. (A10) of Ref. [54], identifying the function $L(s)$ that appears there with $\mathcal{I}_0^{\phi\phi'}(s)/16\pi^2$. The

[6] The IAM cannot be applied naively to the $1/N_C$ expansion, because it leads to a resummation that does not restore two-body unitarity. Thus, if $T = T_{1/N_C} + T_{1/N_C^2} + \cdots$, $T_{\mathrm{IAM}} = T_{1/N_C}^2/(T_{1/N_C} - T_{1/N_C^2})$ does not fulfill the two-body elastic unitarity condition.

definition or extension of the loop function to the SRS is given in Eq. (A13) of the same work.

We decompose the full χPT amplitude matrix $T_{IJ}^{\chi\mathrm{PT}}(s)$ in its $\mathcal{O}(p^2)$ and $\mathcal{O}(p^4)$ contributions (in matrix notation):

$$T_{IJ}^{\chi\mathrm{PT}}(s) = T_{IJ}^{(2)}(s) + T_{IJ}^{(4)}(s) + \mathcal{O}(p^6). \tag{25}$$

The coupled-channel unitarized amplitude is now written as

$$T_{IJ}^{-1}(s) = V_{IJ}^{-1}(s) - \bar{\mathcal{I}}_0(s) - \mathcal{C}_{IJ}, \tag{26}$$

with $\mathcal{C}_{IJ}$ a diagonal matrix of subtraction constants:

$$\mathcal{C}_{IJ} = \mathrm{diag}[C_{IJ}^{\pi\pi}, C_{IJ}^{K\bar{K}}, C_{IJ}^{\eta\eta}] \tag{27}$$

or

$$\mathcal{C}_{IJ} = \mathrm{diag}[C_{IJ}^{K\pi}, C_{IJ}^{K\eta}]. \tag{28}$$

The matrix $V_{IJ}(s)$ is defined such that a chiral expansion of $T_{IJ}(s)$ and $V_{IJ}(s)$ will match the one of $T_{IJ}^{\chi\mathrm{PT}}(s)$. Inverting Eq. (26), we obtain the unitarized matrix $T_{IJ}(s)$:

$$T_{IJ}(s) = [V_{IJ}^{-1}(s) - \bar{\mathcal{I}}_0(s) - \mathcal{C}_{IJ}]^{-1}, \tag{29}$$

$$V_{IJ}(s) = T_{IJ}^{\chi\mathrm{PT}}(s) - T_{IJ}^{(2)}[\bar{\mathcal{I}}_0(s) + \mathcal{C}_{IJ}]T_{IJ}^{(2)}. \tag{30}$$

As already noted in Ref. [52] within the IAM method, the on-shell approximation in the coupled-channel potential has the drawback of generating spurious singularities below the opening of a new channel because the left cut is analytically extrapolated below the inelastic threshold. For instance, as can be appreciated in the top panel of Fig. 2, for $\pi\pi \to \pi\pi$ below the $K\bar{K}$ threshold, the three-loop $\pi\pi \to \bar{K}K \to \bar{K}K \to \pi\pi$ term contains, in the *on-shell* $\bar{K}K \to \bar{K}K$ piece, a 2π-exchange contribution in the t channel, generating a left cut in the partial waves at $s = -4m_\pi^2 + 4m_K^2$ which sits in the elastic scattering region $4m_\pi^2 < s < 4m_K^2$. However, the effect is numerically quite small.

A. $\mathcal{O}(p^4)$ χPT and single-resonance approximation (SRA) amplitudes and large-N_c counting rules

To incorporate LO $1/N_c$ corrections in the description of the interactions among the Goldstone bosons, we follow the scheme derived in [16]. There, the leading-N_c prediction for the actual $\pi\pi$ scattering amplitude was used as deduced from RχT, considering just the lowest-lying nonet of exchanged resonances [11,12].[7] Thus, let us denote by $T_{IJ}^{\mathrm{SRA}}(s)$ the two SU(3)-Goldstone-boson scattering amplitude within the SRA, obtained from the lowest-order RχT Lagrangian [11,12] and projected onto isospin and angular momentum. Below the resonance mass scale, the singularity associated with the pole of a resonance propagator could be replaced by the corresponding momentum expansion; therefore, the exchange of virtual resonances generates derivative Goldstone couplings proportional to powers of $1/m_R^2$. Let us denote by $T_{IJ}^{(4)\mathrm{SRA}}(s)$ the lowest-order term in derivatives. It gives the large-N_c predictions for the $\mathcal{O}(p^4)$ χPT couplings [11,12] and constitutes the leading-$1/N_c$ approximation to $T_{IJ}^{\chi\mathrm{PT}}$. Our approach consists in using Eqs. (29) and (30), but replacing. in the definition of the two-particle-irreducible amplitude, $V_{IJ}(s)$, $T_{IJ}^{\chi\mathrm{PT}}(s)$ by

$$T_{IJ}^{\chi\mathrm{PT}}(s) \leftrightarrow \underbrace{T_{IJ}^{\mathrm{SRA}}(s)}_{\mathcal{O}(1/N_c)} + \underbrace{(T_{IJ}^{\chi PT}(s) - T_{IJ}^{(4)\mathrm{SRA}}(s))}_{\mathcal{O}(1/N_c^2)}. \tag{31}$$

In this way, by construction, we recover the one-loop χPT results, while at the same time, all terms in the amplitude that scale like $1/N_c$ (leading) are also included within the SRA. Note that in the $1/N_c$ counting, the correction $(T_{IJ}^{\chi\mathrm{PT}}(s) - T_{IJ}^{(4)\mathrm{SRA}}(s))$ is incomplete since it does not account for all existing subleading-$1/N_c^2$ contributions to $T_{IJ}(s)$. A complete $1/N_c^2$ calculation would require quantum corrections also stemming from the low-lying resonances.

We should point out a problem that now appears when unitarity is restored. Let us pay attention, for instance, to the ρ exchange, for $\pi\pi \to \pi\pi$ below the $K\bar{K}$ threshold. The $\pi\pi \to \bar{K}K \to \bar{K}K \to \pi\pi$ term contains a contribution from the intermediate $\bar{K}K \to \bar{K}K$ amplitude driven by ρ exchange in the t channel (see bottom panel of Fig. 2). Such a contribution, within the on-shell scheme used here, leads to a spurious left-cut contribution at $s \leq 4m_K^2 - m_\rho^2 \sim (0.64\ \mathrm{GeV})^2$, with very visible consequences if nothing is done. It is indeed unphysical, and it is an artifact of the on-shell unitarization in the coupled

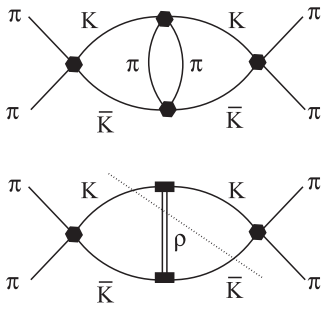

FIG. 2. Some $\mathcal{O}(p^8)$ loop contributions generated when coupled-channels unitarity is restored (Eqs. (29), (30) and (31)). They give rise to pathologies when estimated using anon-shell approximation. In the bottom panel, the line shows a possible source of a physical imaginary part, when the particles cut by it are put on the mass shell.

[7] This latter approximation is justified as long as s, t and u are kept far from the second resonance region.

channels adopted here. A contribution like the one described above cannot physically give rise to an inelastic imaginary part below $s = (2m_K + m_\rho)^2$, as trivially inferred from the optical theorem (see the cut in the figure). In our case we handle the problem by smoothly switching off coupled-channel effects for $\sqrt{s} \leq 0.73$ GeV, and by thus considering purely elastic $\pi\pi \to \pi\pi$ scattering below these energies, where coupled-channel effects are expected to be negligible. The same procedure has been applied to other channels, where similar problems also show up. This problem appears but was not mentioned explicitly in Ref. [30], and it was solved there by reexpanding the ρ-meson propagator as a polynomial, hence removing the singularity. Note that the truncation of the expansion implies that in [30] not all leading-$1/N_c$ terms in the amplitude are included.

V. FITTING STRATEGIES

A. Fitting parameters

Our 24 fitting parameters can be separated into partial-wave specific ones which play the role of renormalization constants,

$$C_{00}^{\pi\pi}, C_{11}^{\pi\pi}, C_{20}^{\pi\pi}, C_{00}^{K\bar{K}}, C_{00}^{\eta\eta}, C_{11}^{K\bar{K}}, \\ C_{\frac{1}{2}0}^{K\pi}, C_{\frac{1}{2}0}^{K\eta}, C_{\frac{1}{2}1}^{K\pi}, C_{\frac{1}{2}1}^{K\eta}, C_{\frac{3}{2}0}^{K\pi}, C_{\frac{3}{2}1}^{K\pi}, \tag{32}$$

and those which appear in the potential:

$$G_V, c_d, c_m, \tilde{c}_d, \tilde{c}_m, d_m, \tilde{d}_m, m_{S_1}, m_{S_8}, m_V, \mu_V, \mu_S. \tag{33}$$

The RχT predictions are supposed to be valid at some fixed value of the renormalization scale, which we allow to be different for vector (μ_V) and scalar (μ_S) couplings.[8]

B. Fitted data and error assignment

An important novelty of this work is the use of the most precise and reliable output for the $\pi\pi$ and πK scattering processes, which is a key factor to attaining high levels of precision and to fix the RχT parameters given in Eq. (33).

[8]The low-lying vector, axial-vector, scalar and pseudoscalar resonances contribute to the L_i (see Table I), where renormalized values L_i^r can be written as a sum $L_i^r = L_i^{\mathrm{SRA}} + \hat{L}_i^r(\mu)$ of the resonance contributions, with a remainder $\hat{L}_i^r(\mu)$. The choice of the renormalization scale μ is arbitrary, and it is common to adopt $\mu = m_\rho$ as a reasonable choice. However, one might take as a best-fit parameter one scale, μ^{RS}, for which a complete resonance saturation of all the LECs L_i^r occurs, that is to say, $\hat{L}_i^r(\mu^{\mathrm{RS}}) = 0$. As suggested in [16], we have considered a scenario where the complete resonance saturation of the LECs L_i^r occurs at two different scales, μ_V for $L_{1,2,9,10}^r$ and μ_S for $L_{4,5,6,8}^r$ depending on whether the LEC is dominated by the vector or the scalar resonance contribution. Note that L_3 and L_7 are renormalization-scale invariant.

In the $\pi\pi$ case, we use the recent data analysis given in [55]. This analysis incorporates the latest data on K_{l4} decays from NA48/2 [56] as well as constraints from Roy equations and one-subtracted coupled dispersion relations—or Garcia-Martin, Kaminski, Pelaez and Yndurain (GKPY) equations. For the πK case, we use the last update of the Roy-Steiner solutions in [57], which includes input from the πK phase shifts around 1.1 GeV and information on the vector πK form factor from tau decays. However, we do not fit to the $\delta_{\frac{3}{2}1}^{\frac{3}{2}1}$ phase shift, as this channel was not considered in the solution of the Roy-Steiner equations, and it came as a prediction of the scheme. Thus, the subtraction constant $C_{\frac{3}{2}1}^{K\pi}$ in Eq. (32) cannot be determined.

In total, the data set which we are fitting is a compilation of 14 independent channels, shown in Table II, from the above two independent sources. Additionally, despite using an elaborated theoretical model to describe these channels, we know that it contains systematic uncertainties (partial resummation) or neglected physics (isospin breaking). A key issue in our fit is therefore how to combine the different experimental and theoretical inputs in a consistent picture.

The first important point is the choice of the data errors for the individual channels. Unfortunately, for the $K\pi$

TABLE II. Compilation of data included in the fit. In the case of the $\pi\pi \to \pi\pi$ channels we take the errors as obtained from the CFD parametrization derived in [55], with two exceptions: in (*) the errors have been multiplied by a factor 2 and the region in the range 990 MeV $< \sqrt{s} <$ 1010 MeV has been excluded from the fit; in (**) the errors have been reduced by a factor of 2.25 (see text for details). The errors on the $\pi\pi \to K\bar{K}$ and $\pi K \to \pi K$ data sets have been obtained from the experimental input uncertainties in [57] (see Figs. 2, 4, 8 and 9 of this reference); however, in the case of $|T^{00}|$ we also added an absolute 0.1 error above 1 GeV. In the last column, we show the contribution χ^2_{chan} of each channel as defined in Eq. (35).

Data set	Range (GeV)	Errors	χ'^2
$\pi\pi \to \pi\pi$ [55]			
δ^{00}	[0.28, 1.2]	(*)	1.6
δ^{11}	[0.28, 1.2]		1.0
δ^{20}	[0.28, 1.2]		0.7
η^{00}	[0.28, 1.2]	(**)	0.5
η^{11}	[0.28, 1.2]		0.0
$\pi\pi \to K\bar{K}$ [57]			
$\lvert T^{00}\rvert$	[0.99, 1.2]	10%	0.8
δ^{00}	[0.99, 1.2]	10%	0.2
$\lvert T^{11}\rvert$	[0.99, 1.2]	10%	0.1
δ^{11}	[0.99, 1.2]	10%	0.0
$\pi K \to \pi K$ [57]			
$\delta_{\frac{1}{2}}^{\frac{1}{2}0}$	[0.64, 1.2]	10%	1.2
$\delta_{\frac{1}{2}}^{\frac{1}{2}1}$	[0.64, 1.2]	10%	0.8
$\delta_{\frac{3}{2}}^{\frac{3}{2}0}$	[0.64, 1.2]	10%	0.4
$\eta_{\frac{1}{2}}^{\frac{1}{2}0}$	[0.64, 1.2]	0.05	0.0
$\eta_{\frac{1}{2}}^{\frac{1}{2}1}$	[0.64, 1.2]	0.05	0.0

scattering, the output of the analysis in Ref. [57] does not provide any errors. Nevertheless, the input contains some experimental uncertainties, typically of the 10% order, and we assume this to be the error for the $K\pi$-scattering data. The only exception is the $|T^{00}|$ case in $\pi\pi \to \bar{K}K$, for which, due to its small value above 1 GeV, we also add 0.1 to the errors. In the case of the $\pi\pi$-scattering channels, we take the errors from the work of Ref. [55] with two exceptions: the δ^{00} phase shift and the η^{00} inelasticity. They are reported to be 1%–5% and about 20%, respectively. Using these errors in a combined fit represents certain difficulties as they are very different compared to all the other channels or the assumptions that entered the model. On the one hand, the sharp error for the δ^{00} would drive the fit to precisely describe this channel at the expense of all the other ones, especially the η^{00}. On the other hand, we do not expect our model to be accurate to a $< 5\%$ level. Therefore, to have a more homogeneous error definition across all channels, we enlarge the reported δ^{00} error by a factor of 2 and divide the reported η^{00} errors by a factor of 2–2.25. The enlargement of the δ^{00} errors is thereby to be interpreted as a quantitative input of the model uncertainties to the fit. Concerning the reweighting of η^{00}, we hope that future, more precise data will make this reweighting unnecessary. In addition, we will see later that the main results of this work are not significantly affected by this choice. Furthermore, our model does not include isospin breaking effects, which are known to play a crucial role in the δ^{00} channel of $\pi\pi \to \pi\pi$ around the region 990 MeV $< \sqrt{s} <$ 1010 MeV. We therefore exclude these data points from the fit.

The second important issue is connected to the pseudo-data points used, as their number in each channel is arbitrary. They are analytically generated from the theoretical analyses carried out in Refs. [55,57], usually in intervals of 5 MeV. To reduce the dependence on this, we normalize each contribution from a given channel by the number of data points in that channel. The exact χ^2 definition is given in the next section. In using this normalized approach, the reduction of the η^{00} errors by 2–2.25 is equivalent to giving an extra weight of 4–5 to this channel in the overall χ^2.

With the above settings we will be able to obtain a consistent fit that homogeneously describes all 14 channels and is compatible with the theoretical assumptions entering the model.

C. The usual χ^2 approach

On the one hand, a fit to the scattering data of the $N_{dc} = 14$ channels involves the standard χ^2, defined as

$$\chi^2_{\rm exp} = N_d \sum_{\rm chan=1}^{N_{dc}} \chi^2_{\rm chan}, \tag{34}$$

$$\chi^2_{\rm chan} = \frac{1}{n}\sum_{i=1}^{n}\left(\frac{O_i^{\rm th} - O_i^{\rm exp}}{\Delta O_i^{\rm exp}}\right)^2, \tag{35}$$

with N_d the overall total number of data points. The $(O_i^{\rm exp}, \Delta O_i^{\rm exp})$ are the fitted observables with their corresponding errors, and $O_i^{\rm th} = F_i(p, C)$ are our theoretical descriptions, with $p_j = G_V, c_d, \ldots$ parameters subjected to theoretical conditions and $C_j = C_{00}^{\pi}, \ldots$ parameters which *can only* be determined from data. On the other hand, we typically expect our calculation to be accurate up to $1/N_c$ corrections. Thus, if a fit turns out to provide numbers completely different from the large-N_c estimates of Eqs. (8) and (9), we will suspect the fit. The optimal situation would be when the data have an accuracy able to reliably pin down all the parameters. Unfortunately, this is *not* the case. Attempts to determine the C_{IJ} subtraction constants in Eq. (32) *and* the RχT parameters in Eq. (33) (in all 23 parameters) produce multiple minima with at times quite unreasonable values for the RχT parameters. In this case, we are inclined to reject the fit. If, on the other hand, the large-N_c constraints are fully implemented[9] and larger error bands are assumed, the resulting fits are likewise not satisfactory.

We want to obtain a *reasonable* fit with *sensible* parameters. Therefore, rather than expecting the fit to tell us *a posteriori* whether the parameters are reasonable, we provide *a priori* a reasonable guess for the parameters and search for the minimum within the expected departure of this assumption. In the next section, we explain how we include the *a priori* input in the fit.

The existence of multiple solutions is a consequence of several shallow directions in the parameter space, which makes it impossible to identify a unique global minimum. This situation could be solved by including further experimental or theoretical information, for example, data of those channels that, considered in the coupled-channel formalism, have not been fitted. Unfortunately, this is not the case, and a Bayesian fit with large-N_c priors becomes a natural and simple way to circumvent this problem.

Guo and Oller [30] handle the problem of proliferation of parameters in a different manner. They took free values for all the resonance parameters (p_j in our notation), but they invoked some *unclear* SU(3) relations among the subtraction constants (C_j in our notation) and kept just four independent. However, this is not a consistent approach. First, the subtraction constants are not, in principle, related by SU(3) and should all be taken as independent (see discussion in [17]). Second, the unconstrained fit of the resonance parameters to data leads, in some cases, to values in clear contradiction to the large-N_c expectations.[10] Conversely, the Bayesian approach to be discussed below, where large-N_c constraints are imposed as a probabilistic prior, does not support the assumptions of Ref. [30].

[9] As done in the previous work [16] with a lower-energy cutoff $\sqrt{s} \lesssim 700$ MeV.

[10] For instance, a best-fit value of 15 MeV for c_d was obtained in [30], which is around a factor of 3 smaller than that of $f_\pi/2$ given in Eq. (8)

D. The augmented χ^2 approach

In the Bayesian interpretation, the fitting parameters are actually random variables which are determined from the existing data and a prior probability of finding the parameters, regardless of the actual measurements under analysis. We shall not dwell on the philosophical intricacies, and we use the augmented χ^2 method to fix the prior distribution [58–60]. This approach has successfully been used in lattice QCD to analyze a number of data with a similar number of parameters. In our case the situation is slightly different, but we expect the large-N_c limit to set reasonable ranges on the fitting parameters.

We consider first the theoretical χ^2 defined in Eq. (13). This figure of merit is coherent with the assumption that the prior probability for the RχT parameters is given by their large-N_c estimate, within a relative $1/N_c$ accuracy (and *not* as a uniform distribution). We use the results of Eq. (8) for $G_V, \tilde{c}_m, c_d, \tilde{c}_d, d_m, \tilde{d}_m$ and Eq. (9) for m_{S_0}, m_{S_8}, m_V. Thus, we take the following Gaussian variables normalized to the *same* $\Delta p_i = f_\pi/N_c$:

$$\xi_{G_V} = \frac{\sqrt{2}G_V - f_\pi}{f_\pi/N_c}, \qquad \xi_{c_d} = \frac{2c_d - f_\pi}{f_\pi/N_c}, \ldots$$
$$\xi_{m_V} = \frac{\sqrt{N_c/24\pi^2}m_V - f_\pi}{f_\pi/N_c}, \ldots \tag{36}$$

We provide, in addition, an *a priori* splitting $m_{S_0} - m_{S_8}$ for the scalar octet and singlet masses, which are equal at large N_c:

$$\xi_{m_{S_0}-m_{S_8}} = \sqrt{\frac{N_c}{24\pi^2}}\frac{m_{S_0} - m_{S_8}}{f_\pi/N_c}, \tag{37}$$

and we finally also consider the robust constraint in the large-N_c limit $4c_d c_m \sim f_\pi^2$, obtained by requiring the $K\pi$ scalar form factor to vanish in the $t \to \infty$ limit [61],

$$\xi_{c_d c_m} = \frac{\sqrt{4c_d c_m} - f_\pi}{f_\pi/N_c}. \tag{38}$$

Thus, we take into account a total of 10 contributions to construct $\chi^2_{\rm th}$,

$$\chi^2_{\rm th} = [\xi^2_{G_V} + \xi^2_{c_d} + \xi^2_{c_d c_m} + \xi^2_{d_m} + \xi^2_{\tilde{c}_d} + \xi^2_{\tilde{c}_m} + \xi^2_{\tilde{d}_m}] + [\xi^2_{m_V} + \xi^2_{m_{S_8}} + \xi^2_{m_{S_0}-m_{S_8}}]. \tag{39}$$

In addition, we take, for the singlet and octet pseudoscalar resonance masses, $m_{P_i} = \sqrt{2}m_{S_i}, i = 0, 8$ (see Sec. II).

The key question now is how to combine $\chi^2_{\rm exp}$ and $\chi^2_{\rm th}$. Obviously, since we have a small number of constraints N_p as compared to the number of data or pseudodata N_d, a direct addition of $\chi^2_{\rm exp}$ and $\chi^2_{\rm th}$ would make the constraints irrelevant. Therefore, we will construct a *reduced* χ^2, $\bar{\chi}^2 \equiv \chi^2/N$, with a 50% weighting on the data or pseudodata and the theoretical constraints.

Thus, we define

$$\chi^2_{\rm total} = \frac{N_d + N_p}{2}\left(\frac{\chi^2_{\rm exp}}{N_d N_{dc}} + \frac{\chi^2_{\rm th}}{N_p}\right). \tag{40}$$

The additional terms in the total χ^2 impose a penalty for fits which deviate from the large-N_c expectations by more than $1/N_c$. This is just a condition on the naturalness of parameters, based on a simple large-N_c estimate. Of course, the values we are taking as a reference are based just on the single-resonance approximation, and this is precisely why one should not attach exaggerated significance to the detailed accuracy of the reasonable fit. The opposite situation, the impossibility of performing a successful fit, would signal a serious drawback of the whole framework, including the usefulness of the short-distance constraints in meson-meson scattering.

Furthermore, we have checked our approach against the weighting choice of Eq. (40). We found that the parameters in Table III do not depend strongly on this particular setting as long as the fit starts in the vicinity of the respective minimum. That is, the augmentation of Eq. (40) is needed to isolate the physical minimum of Table III from all the unphysical local minima, but after having found it, the corresponding parameters do not strongly depend on the specific choice of Eq. (40).

E. Results

The values of the fitted parameters are presented in Table III, and the results for scattering properties are

TABLE III. Parameters (in MeV) of the RχT Lagrangian determined from phenomenology [11,12] or short-distance constraints [14] and the resulting values from the combined fit. Resonance masses and saturation scales are also given in MeV, while subtraction constants are dimensionless.

Parameter	Large N_c	Fit		Fit
G_V	65.3	63.2(1)	$C_{00}^{\pi\pi}$	−0.0209(2)
c_d	46.2	39.8(1)	$C_{00}^{K\bar{K}}$	−0.0085(3)
$\tilde{c}_d$	26.7	20.7(3)	$C_{00}^{\eta\eta}$	0.0060(2)
c_m	46.2	41.1(1)	$C_{11}^{\pi\pi}$	−0.0279(6)
$\tilde{c}_m$	26.7	18.9(9)	$C_{11}^{K\bar{K}}$	−0.0100(5)
d_m	32.7	29.8(1)	$C_{20}^{\pi\pi}$	−0.0561(5)
$\tilde{d}_m$	18.9	19.3(7)	$C_{\frac{1}{2}0}^{K\pi}$	−0.0029(3)
m_V	821	805(2)	$C_{\frac{1}{2}0}^{K\eta}$	−0.0165(14)
m_{S_0}	821.0	808.9(4)	$C_{\frac{1}{2}1}^{K\pi}$	0.0380(20)
m_{S_8}	821	1279(9)	$C_{\frac{1}{2}1}^{K\eta}$	−0.0240(20)
μ_V		645(4)	$C_{\frac{3}{2}0}^{K\pi}$	−0.0394(14)
μ_S		274(10)	$C_{\frac{3}{2}1}^{K\pi}$	–

depicted in Fig. 3, where solid (blue) lines represent fitted curves. The results for nonfitted data are depicted as dashed (blue) lines. In the Bayesian approach, errors on the parameters are estimated as *mean* values, i.e., integrating the likelihood with respect to the fitting parameters, but when the total χ^2 is large (not the χ^2/d.o.f.), as is the case here, a saddle-point approximation can be used. This is equivalent to determining them by the standard covariance matrix inversion method applied in our case to Eq. (40).

As expected, the fit below $\Lambda_R = 1.2$ GeV is successful with reasonable resonance parameters motivated by large-N_c constraints (when states with mass above Λ_R are disregarded). Indeed, as can be seen in Table III, all RχT parameters turn out to be in agreement, within the typical 30% uncertainty, with the large-N_c expectations. The only exception is the value of $m_{S_8} \sim 1280$ MeV, which lies outside of the N_c expected region. However, the mean between the two scalar masses, m_{S_8} and m_{S_0}, satisfies this constraint.

The achieved description for all 14 *pseudodata* channels considered is quite good, as can be appreciated in Fig. 3. This is even more relevant, taking into account that the comparison is being made with the quite precise output obtained from the data constrained Roy-GKPY and Roy-Steiner analyses carried out in Refs. [55,57], which provide the most reliable information currently available in the literature on the various scattering amplitudes.

Next, we discuss the poles found in the SRS of the amplitudes. The SRS of the T matrix is determined by the definition of the loop function $\mathcal{I}_0^{\phi\phi'}(s)$. As mentioned above, we use Eq. (A13) of Ref. [54]. Masses and widths of the dynamically generated resonances are determined from the positions of the poles, s_R, in the SRS of the corresponding scattering amplitudes in the complex s plane. Since in the SRA amplitudes we have explicitly incorporated one vector and two scalar poles, we expect at least these poles to appear in the appropriate sectors. However, because of the resummation in Eq. (29), the pole positions will change with respect to those of the bare ones ($s = m_V^2, m_{S_0}^2$ and $m_{S_8}^2$) and the resonances will acquire a width that accounts for their two-meson decay. This change is especially relevant for the $f_0(500)$ or σ

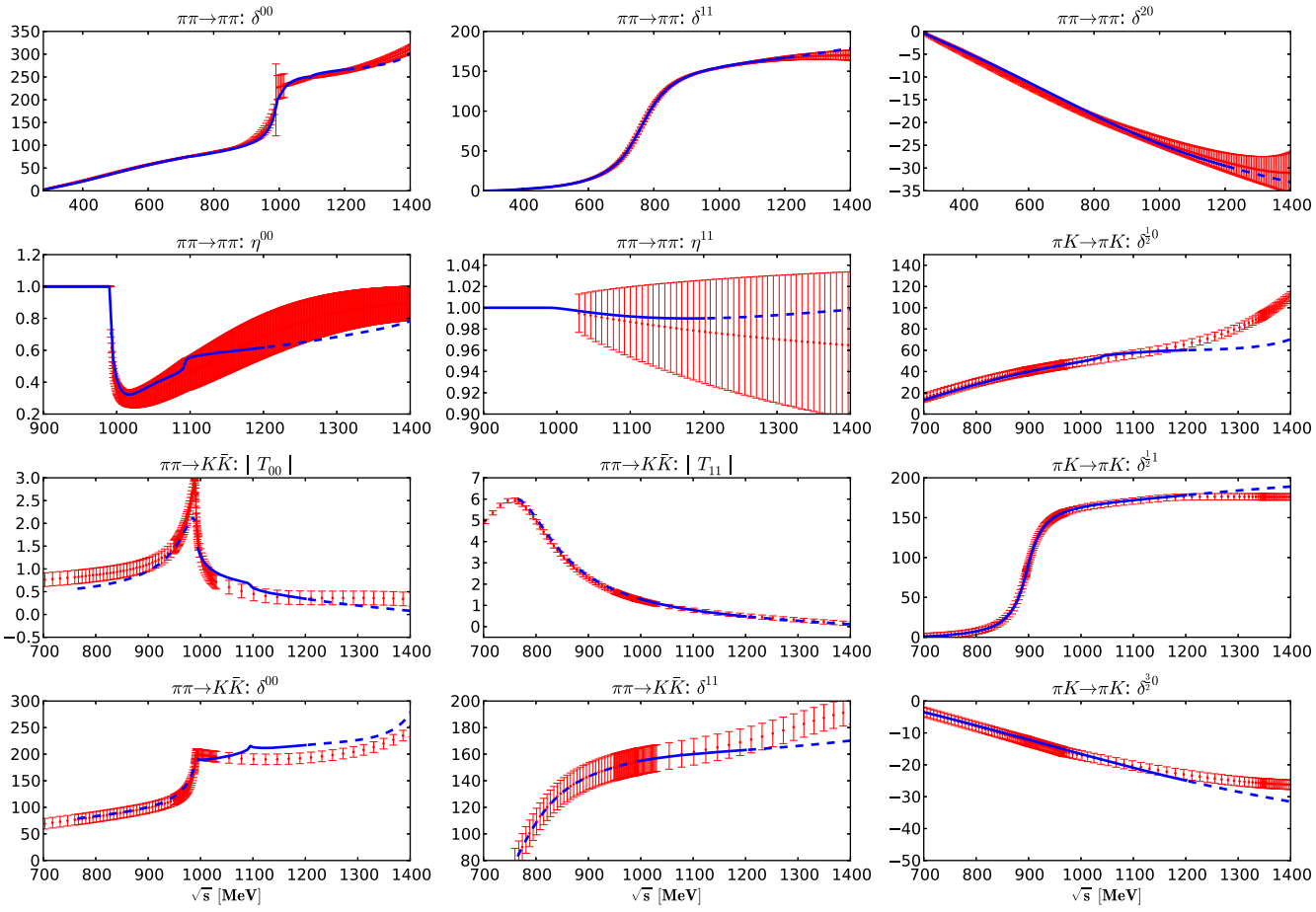

FIG. 3 (color online). Results for meson-meson scattering observables as a function of the CM energy $\sqrt{s}$ (in MeV). We display the pseudodata, with their assumed uncertainties included in the fit (see Table II). Solid lines represent fitted curves; dashed (blue) lines represent nonfitted curves.

TABLE IV. Pole positions and resonance couplings found in this work with the best-fit parameters compiled in Table III. All statistical uncertainties are defined on a 68% confidence level. For the resonances marked with (*), the PDG quote Breit-Wigner (BW) parameters $s_{\rm pole} = M_{\rm BW}^2 - iM_{\rm BW}\Gamma_{\rm BW}$, from which we have computed the corresponding pole positions. For the $\rho(770)$ case we show the "Neutral only, other reactions" average values, whereas for the $K^*(892)$ case we give the "Neutral only" average mass and width. Note that the dispersive data analysis of Ref. [64], based on the Roy equations, predict $\sqrt{s_\sigma} = (441^{+16}_{-8} - i272^{+9}_{-12})$ MeV. In addition, the $|g_{\pi\pi}|$ GKPY dispersive determination given in [62] for the $f_0(500)$, $f_0(980)$ and $\rho(770)$ are $3.59^{+0.11}_{-0.13}$, 2.3 ± 0.2 and $6.01^{+0.04}_{-0.07}$, respectively.

I	J		$\sqrt{s_R}$ [MeV]	$\lvert g_{\pi\pi,\pi K}\rvert$ [GeV]	$\lvert g_{\bar{K}K}\rvert$ [GeV]	PDG [43] $\sqrt{s_R}$ [MeV]	GKPY/RS [62,63] $\sqrt{s_R}$ [MeV]
0	0	$f_0(500)$ or σ	$458(2) - i264(3)$	3.3(1)	0.9(1)	$400 \sim 550 - i[200 \sim 350]$	$457^{+14}_{-13} - i279^{+11}_{-7}$
0	0	$f_0(980)$	$1001(4) - i24(2)$	2.2(1)	4.2(1)	$990 \pm 20 - i[20 \sim 50]$	$996(7) - i25^{+10}_{-6}$
0	0		$1211(64) - i332(78)$	3.3(5)	2.6(2)		
0	0		$1449(29) - i61(12)$	3.1(2)	0.3(1)		
1	1	$\rho(770)$	$761(3) - i73(2)$	6.0(1)	3.9(1)	$772.3(9) - i75.1(8)^*$	$763.7^{+1.7}_{-1.5} - i73.2^{+1.0}_{-1.1}$
1/2	0	$K_0^*(800)$ or κ	$684(4) - i260(4)$	4.2(1)		$682(29) - i273(12)$	$659(13) - i278(12)$
1/2	1	$K^*(892)$	$897(5) - i24(2)$	5.4(3)		$896.1(19) - i23.7(3)^*$	

meson, where pion loops dominate at $N_c = 3$, producing a state very deep on the complex plane, with a mass around 450 MeV and a width around 520 MeV. As studied in [33], this effect is due to a strong cancellation between different N_c orders, which makes it difficult to analyze its properties just from the pure $1/N_c$ expansion. In fact, there are several works in the literature [16,28–32] in which the $f_0(500)$ fades away on the complex plane as N_c increases, being made just of meson-meson loops and having, then, no relation with the scalar poles included in the Lagrangian.

In addition, as we will see, some other poles are generated as well in the SRS of the scattering amplitudes. The results are presented in Table IV. We find a quite good description of the $f_0(500), f_0(980), K_0^*(800), \rho(770)$ and $K^*(892)$ resonances, with masses and widths that compare rather well with the averaged ones compiled in the Review of Particle Properties [43]. Furthermore, since our results have been obtained by fitting the pseudodata values from the $\pi\pi$ [55] and πK [57] dispersive analyses, we also include, in the last row of Table IV, the dispersive determinations obtained from these schemes [62,63]. The agreement is also remarkable. We want to note that the properties of all these dynamically generated states are not significantly affected by the employed reweighting of the δ^{00} and η^{00} channels.

Let us now pay attention to the complex pole structure of the scalar-isoscalar sector, depicted in Fig. 4. The $f_0(500)$ and $f_0(980)$ resonances are clearly visible. Besides, there are two additional poles, which are placed above $\Lambda_R = 1.2$ GeV. Perhaps the lower one could have some relation with the $f_0(1370)$ state. This will agree with the findings of Ref. [65], where the $f_0(1370)$ is identified as a pure octet state not mixed with the glueball. The chiral unitary approaches, supplemented by the inclusion of vector mesons, of Refs. [66–68] seem to also give support to this hypothesis. Nevertheless, the exact position of the higher poles depends much more on the choice of the merit function which is being minimized. In particular, the position of the $f_0(1370)$ depends strongly on how the comparatively imprecise η^{00} pseudodata is included in the fit. In addition, these states are located above the scale of the first resonance multiplet considered and, then, are strongly dependent on those heavier states integrated out in the starting Lagrangian. Therefore, these heavier poles cannot be properly described within the framework used in this work and are included only for completeness.

Finally, in Table IV, we also provide for each resonance its coupling to the fitted channels [πK in the case of the $K_0^*(800)$ and $K^*(892)$, and $\pi\pi$ and KK for the others], defined from its pole residue as

$$g_A g_B = \lim_{s \to s_{\rm pole}} (s - s_{\rm pole}) T_{IJ}^{A \to B}(s)(2J+1)/(2p)^{2J}, \quad (41)$$

where p is the center-of-mass-system momentum of the corresponding process.

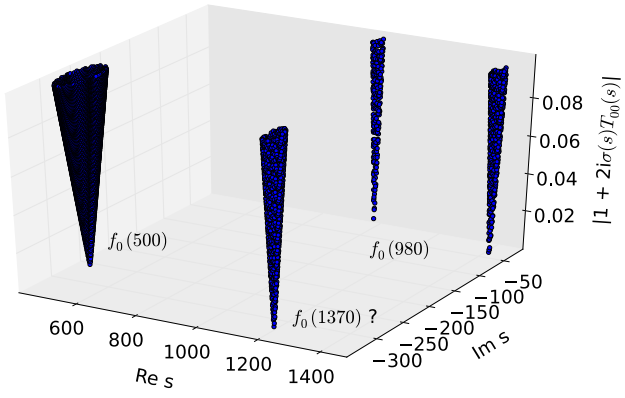

FIG. 4 (color online). Poles found in the SRS of the scalar-isoscalar elastic $\pi\pi$ amplitude. The $f_0(500)$ and $f_0(980)$ are clearly visible.

VI. CONCLUSIONS

Within a unitarized coupled-channel approach, we have analyzed the scattering of the pseudoscalar mesons for $\sqrt{s} \leq 1.2$ GeV, where all two-body scattering channels are open. Our amplitudes contain one-loop (NLO) χPT and tree-level (LO) large-N_c pieces, with 24 fitting parameters. Given the lack of very precise experimental data, in this work we have used the most precise and reliable output for the $\pi\pi$ and πK scattering processes from the Roy-GKPY and Roy-Steiner analyses carried out in Refs. [55,57]. This is a major novelty of this work, since for the very first time, these two sets of data or pseudodata have been simultaneously used to constrain the LECs. Indeed, it has been a key factor to attaining high levels of precision and to fixing the RχTT parameters. However, not all of the pseudodata have experimentally inherited uncertainties, and hence an educated guess in defining the merit function used has been made.

While our model contains important features of the true solution and we optimized it by minimizing the discrepancies with *experiment*, the large number of best-fit parameters made the task of performing the fit difficult. We faced a quite complex structure of the parameter manifold, which has many resemblances to a multidimensional egg box. The proliferation of undetermined LECs made direct fits rather elusive, and quite often we were driven to unreasonable parameter values, which suggested rejecting the fit. Under these circumstances, we have adopted the Bayesian point of view of making the natural assumption that the RχT parameters take their large-N_c estimated values within an expected $1/N_c$ uncertainty.

The main outcome of the present study is that a rather good description of the data can be achieved with natural values of the parameters and by considering the nominal expected accuracy of the calculations. This is a nontrivial result, and an important ingredient for this success is the allowance for systematic deviations in all parameters where the large-N_c expansion is expected to provide corrections of $\mathcal{O}(1/N_c)$. The predictions compiled in Table IV for pole positions and couplings of the lowest-lying dynamically generated resonances, which show a nice agreement with the most precise current determinations, are an example of this success.

ACKNOWLEDGMENTS

We thank B. Moussallam for the results of the update of his Roy-Steiner dispersive analysis of πK scattering and Z. H. Guo for discussions on the approach employed in Ref. [30]. We also acknowledge useful discussions with M. Albaladejo. This work has been supported in part by the Spanish Government and ERDF funds from the EU Commission [Grants No. FIS2011-24149, No. FIS2011-28853-C02-01, No. FIS2011-28853-C02-02, No. FPA2011-23778 and No. CSD2007-00042 (Consolider Project CPAN)], Generalitat Valenciana (Grants No. PROMETEO/2009/0090 and No. PROMETEOII/2013/007), Junta de Andalucía (Grant No. FQM225), the DFG (SFB/TR 16, "Subnuclear Structure of Matter") and the EU Hadron-Physics3 project (Grant No. 283286).

APPENDIX: SRA RχT AND ONE-LOOP χPT AMPLITUDES

The $\mathcal{O}(p^4)$ χPT amplitudes $[T_{IJ}^{\chi\mathrm{PT}}(s)]$ used throughout this work are obtained from Ref. [52]. There, and assuming crossing symmetry, the isospin projected amplitudes for every possible process involving π, K, η mesons can be found. Next, the individual contributions with total angular momentum J are calculated using Eq. (17). Possible $\eta - \eta'$ mixing effects are not taken into account, and thus the η meson is identified with the isospin singlet (η_8) of the octet of Goldstone bosons. In addition, the normalizations used here are such that our amplitudes differ in one sign from those given in [52].

(i) $\pi\pi \to \pi\pi$: There is only one independent amplitude, $T(s,t,u)$, that is taken to be the $\pi^+\pi^- \to \pi^0\pi^0$, which at one loop in χPT, is given in Eq. (B4) of Ref. [52]. Linear combinations of $T(s,t,u)$, $T(t,s,u)$ and $T(u,t,s)$ provide the isoscalar, isovector and isotensor amplitudes [see text above Eq. (12) in [52]].

(ii) $K\pi \to K\pi$: Crossing symmetry allows us to write the $I = 1/2$ amplitude [Eq. (12) in [52]] in terms of the $I = 3/2$ $K^+\pi^+ \to K^+\pi^+$ one, which is given in Eq. (B5) of Ref. [52].

(iii) $K\bar{K} \to K\bar{K}$: In this case, the two isospin amplitudes can be expressed in terms of the $\bar{K}^0K^0 \to K^+K^-$ amplitude [see Eq. (25) of Ref. [30]], an expression which to one loop can be obtained from Eq. (B8) of [52]. Note that this latter equation suffers from a typo, and there, it turns out that the amplitude $K^0\bar{K}^0 \to K^+K^-$ is the one which is given instead of $\bar{K}^0K^0 \to K^+K^-$.

(iv) $K\bar{K} \to \pi\pi$: Thanks to crossing symmetry, the amplitudes in this sector are determined by the $I = 3/2$ $K^+\pi^+ \to K^+\pi^+$ one.

(v) $K\eta \to K\eta$: This is a pure $I = 1/2$ process. The one-loop amplitude is given in Eq. (B2) of Ref. [52].

(vi) $\bar{K}K \to \eta\eta$: This is an $I = 0$ process that, using crossing symmetry, can be obtained from the previous amplitude.

(vii) $K\eta \to K\pi$: This is also an $I = 1/2$ process, and the one-loop expression for $\bar{K}^0\eta \to K^0\pi^0$ can be found in Eq. (B3) of Ref. [52].

(viii) $KK \to \pi\eta$: This $I = 1$ process is related to the $\bar{K}^0\eta \to K^0\pi^0$ amplitude by crossing symmetry.

(ix) $\pi\eta \to \pi\eta$: This is a pure $I = 1$ isospin process, and its amplitude is given in Eq. (B6) of Ref. [52].

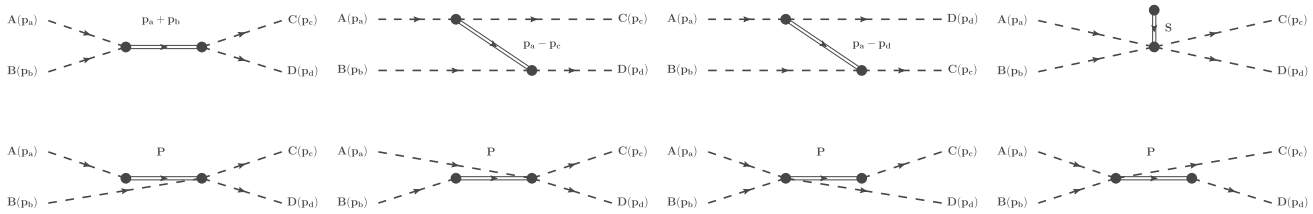

FIG. 5. Resonance contributions to the pseudoscalar meson-meson scattering. The dotted lines denote pseudoscalar mesons, double lines the intermediate resonances, and the black dot their interaction. The first row contains the diagrams with intermediate vector and scalar resonances in the s-, t- and u-channel graphs. The pseudoscalar resonance contributions are shown in the second row.

(x) $\pi\pi \to \eta\eta$: This amplitude is determined from the previous one by crossing.

(xi) $\eta\eta \to \eta\eta$: This pure $I = 0$ amplitude at one loop in χPT is given in Eq. (B1) of Ref. [52].

Next, we compile the RχT amplitudes $T^{\rm SRA}(s,t,u)$, within the SRA, for the independent processes mentioned above. The different Feynman diagrams corresponding to the resonance exchange amplitudes are illustrated in Fig. 5. Note that, as it has been anticipated in Eq. (31), tree-level amplitudes are also included in $T^{\rm SRA}(s,t,u)$. In addition, resonances contribute indirectly through the diagrams of Fig. 6 which modify, at $\mathcal{O}(p^4)$, the pion-decay constant and the pseudoscalar meson self-energy $\Sigma^R_{\phi=\pi,K,\eta}(p^2)$ and, consequently, pseudoscalar masses and wave-function renormalization constants. The scalar and pseudoscalar resonance contribution to the pion-decay constant and self-energy renormalization reads

$$
\begin{aligned}
f_\pi &= f\left(1+\frac{8}{3}\frac{c_m c_d}{f^2 m_{S_8}^2}(m_\pi^2-m_K^2)+4\frac{\tilde{c}_m\tilde{c}_d}{f^2 m_{S_0}^2}(2m_K^2+m_\pi^2)\right),\\
\Sigma_\pi^S(p^2) &= \frac{-16c_m(m_\pi^2-m_K^2)}{3f^2 m_{S_8}^2}[c_d p^2 - c_m m_\pi^2] - \frac{8\tilde{c}_m(2m_K^2+m_\pi^2)}{f^2 m_{S_0}^2}[\tilde{c}_d p^2 - \tilde{c}_m m_\pi^2],\\
\Sigma_K^S(p^2) &= \frac{-8c_m(m_\pi^2-m_K^2)}{3f^2 m_{S_8}^2}[-c_d p^2 + c_m m_K^2] - \frac{8\tilde{c}_m(2m_K^2+m_\pi^2)}{f^2 m_{S_0}^2}[\tilde{c}_d p^2 - \tilde{c}_m m_K^2],\\
\Sigma^P_{\phi=\pi,K}(p^2) &= 8\frac{d_m^2 m_\phi^4}{f^2}\frac{1}{p^2-m_{P_8}^2}, \qquad \Sigma_\eta^S(p^2) = \frac{4}{3}\Sigma_K^S(p^2) - \frac{1}{3}\Sigma_\pi^S(p^2).
\end{aligned}
\tag{A1}
$$

Therefore, taking into account all these contributions, the $T^{\rm SRA}(s,t,u)$ amplitude for the channel $\pi^+\pi^- \to \pi^0\pi^0$ is given by

$$
\begin{aligned}
T^{\rm SRA}(s,t,u) &= \frac{1}{f_\pi^2}(m_\pi^2-s) + \frac{G_V^2}{f_\pi^4}\left(\frac{t(s-u)}{t-m_V^2}+\frac{u(s-t)}{u-m_V^2}\right) + \frac{2(2c_m m_\pi^2 + c_d(-2m_\pi^2+s))^2}{3f_\pi^4(s-m_{S_8}^2)}\\
&\quad + \frac{4(2\tilde{c}_m m_\pi^2 + \tilde{c}_d(-2m_\pi^2+s))^2}{f_\pi^4(s-m_{S_0}^2)} - \frac{8m_\pi^4 d_m^2}{f_\pi^4(m_\pi^2-m_{P_8}^2)}.
\end{aligned}
\tag{A2}
$$

For the channel $K^+\pi^+ \to K^+\pi^+$,

$$
\begin{aligned}
T^{\rm SRA}(s,t,u) &= \frac{1}{2f_\pi^2}(s-m_K^2-m_\pi^2) - \frac{G_V^2}{2f_\pi^4}\left\{\frac{t(s-u)}{t-m_V^2} + \frac{(t-2m_K^2)(t-2m_\pi^2)-(m_K^2+m_\pi^2-s)^2}{u-m_V^2}\right\}\\
&\quad + \frac{4(2(-\tilde{c}_d+\tilde{c}_m)m_K^2+\tilde{c}_d t)(2(-\tilde{c}_d+\tilde{c}_m)m_\pi^2+\tilde{c}_d t)}{f_\pi^4(t-m_{S_0}^2)} + \frac{((c_d-c_m)(m_K^2+m_\pi^2)-c_d u)^2}{f_\pi^4(u-m_{S_8}^2)}\\
&\quad - \frac{(2(c_d-c_m)m_K^2-c_d t)(2(c_d-c_m)m_\pi^2-c_d t)}{3f_\pi^4(t-m_{S_8}^2)} - \frac{4d_m^2 m_\pi^2 m_K^2}{f_\pi^4}\left(\frac{1}{m_K^2-m_{P_8}^2}+\frac{1}{m_\pi^2-m_{P_8}^2}\right)\\
&\quad + \frac{c_m(m_K^2-m_\pi^2)(3c_m(m_K^2-m_\pi^2)+c_d(4m_K^2+4m_\pi^2-5s+t+u))}{3f_\pi^4 m_{S_8}^2}.
\end{aligned}
\tag{A3}
$$

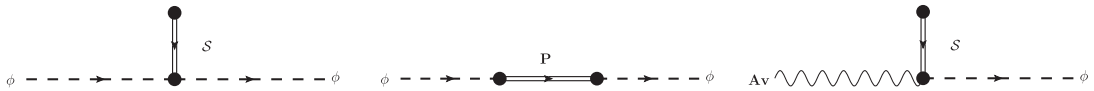

FIG. 6. Scalar and pseudoscalar resonance contributions to the pseudoscalar meson self-energy and the scalar one to the pion decay constant f_π.

For $K^0\bar{K}^0 \to K^+K^-$ the SRA amplitude reads

$$T^{\mathrm{SRA}}(s,t,u) = \frac{u-2m_K^2}{2f_\pi^2} + \frac{G_V^2}{2f_\pi^4}\left(\frac{s(t-u)}{s-m_V^2} + \frac{t(s-u)}{t-m_V^2}\right) + \frac{4(2\tilde{c}_m m_K^2 + \tilde{c}_d(-2m_K^2+s))^2}{f_\pi^4(s-m_{S_0}^2)} - \frac{(2c_m m_K^2 + c_d(-2m_K^2+s))^2}{3f_\pi^4(s-m_{S_8}^2)} + \frac{(2c_m m_K^2 + c_d(-2m_K^2+t))^2}{f_\pi^4(t-m_{S_8}^2)} - \frac{8d_m^2 m_K^4}{f_\pi^4(m_K^2-m_{P_8}^2)} + \frac{4c_d c_m(m_K^2-m_\pi^2)(2m_K^2-u)}{f_\pi^4 m_{S_8}^2}, \tag{A4}$$

whereas for the process $\bar{K}^0\eta \to \bar{K}^0\eta$,

$$\begin{aligned} T^{\mathrm{SRA}}(s,t,u) = {} & \frac{-9t+6m_\eta^2+2m_\pi^2}{12f_\pi^2} - \frac{3G_V^2}{4f_\pi^4}\left\{\frac{((t-2m_K^2)(t-2m_\eta^2)-(m_K^2+m_\eta^2-u)^2)}{(s-m_V^2)}\right. \\ & \left. + \frac{((t-2m_K^2)(t-2m_\eta^2)-(m_K^2+m_\eta^2-s)^2)}{(u-m_V^2)}\right\} - \frac{(c_m(-5m_K^2+3m_\pi^2)+c_d(m_\eta^2+m_K^2-s))^2}{6f_\pi^4(m_{S_8}^2-s)} \\ & + \frac{(2(c_d-c_m)m_K^2-c_d t)(2c_m(8m_K^2-5m_\pi^2)+3c_d(-2m_\eta^2+t))}{9f_\pi^4(m_{S_8}^2-t)} - \frac{(c_m(-5m_K^2+3m_\pi^2)+c_d(m_\eta^2+m_K^2-u))^2}{6f_\pi^4(m_{S_8}^2-u)} \\ & - \frac{4(2(-\tilde{c}_d+\tilde{c}_m)m_K^2+\tilde{c}_d t)(-6\tilde{c}_d m_\eta^2+8\tilde{c}_m m_K^2-2\tilde{c}_m m_\pi^2+3\tilde{c}_d t)}{3f_\pi^4(m_{S_0}^2-t)} \\ & + \frac{4d_m^2(-4m_K^4+3m_\pi^2m_K^2)}{3f_\pi^4(m_K^2-m_{P_8}^2)} + \frac{4d_m^2(-20m_K^4+9m_\pi^2m_K^2-4m_\pi^4)}{9f_\pi^4(m_\eta^2-m_{P_8}^2)} - \frac{32\tilde{d}_m^2(2m_K^4-3m_\pi^2m_K^2+m_\pi^4)}{3f_\pi^4(m_\eta^2-m_{P_0}^2)} \\ & + \frac{c_m(m_K^2-m_\pi^2)(21c_m(-m_K^2+m_\pi^2)+c_d(246m_K^2-58m_\pi^2-63(s+u)))}{9f_\pi^4 m_{S_8}^2}. \end{aligned} \tag{A5}$$

For the channel $\bar{K}^0\eta \to \bar{K}^0\pi^0$ we have

$$\begin{aligned} T^{\mathrm{SRA}}(s,t,u) = {} & -\frac{8m_K^2+m_\pi^2+3m_\eta^2-9t}{12\sqrt{3}f_\pi^2} - \frac{\sqrt{3}G_V^2\{(m_K^2+m_\pi^2-u)(m_K^2+m_\eta^2-u)-(2m_K^2-t)(m_\pi^2+m_\eta^2-t)\}}{4f_\pi^4(s-m_V^2)} \\ & - \frac{\sqrt{3}G_V^2\{(m_K^2+m_\pi^2-s)(m_K^2+m_\eta^2-s)-(2m_K^2-t)(m_\pi^2+m_\eta^2-t)\}}{4f_\pi^4(u-m_V^2)} \\ & + \frac{(c_m(-5m_K^2+3m_\pi^2)+c_d(m_\eta^2+m_K^2-s))((c_d-c_m)(m_K^2+m_\pi^2)-c_d s)}{2\sqrt{3}f_\pi^4(-m_{S_8}^2+s)} \\ & + \frac{(-2c_m m_\pi^2+c_d(m_\eta^2+m_\pi^2-t))(2(c_d-c_m)m_K^2-c_d t)}{\sqrt{3}f_\pi^4(m_{S_8}^2-t)} \\ & + \frac{(c_m(-5m_K^2+3m_\pi^2)+c_d(m_\eta^2+m_K^2-u))((c_d-c_m)(m_K^2+m_\pi^2)-c_d u)}{2\sqrt{3}f_\pi^4(u-m_{S_8}^2)} \\ & + \frac{16\tilde{d}_m^2(-2m_K^4+m_K^2m_\pi^2+m_\pi^4)}{3\sqrt{3}f_\pi^4(m_\eta^2-m_{P_0}^2)} + \frac{4d_m^2m_K^2(-2m_K^2+m_\pi^2)}{\sqrt{3}f_\pi^4(m_K^2-m_{P_8}^2)} \\ & + \frac{2d_m^2(4m_K^4-5m_K^2m_\pi^2+m_\pi^4)}{9\sqrt{3}f_\pi^4(m_\eta^2-m_{P_8}^2)} + \frac{2d_m^2m_\pi^2(-3m_K^2+m_\pi^2)}{3\sqrt{3}f_\pi^4(m_\pi^2-m_{P_8}^2)} \\ & + \frac{c_m(m_K^2-m_\pi^2)(c_m(-m_K^2+m_\pi^2)+c_d(8m_K^2-8m_\pi^2+4s-11t+4u))}{3\sqrt{3}f_\pi^4 m_{S_8}^2}. \end{aligned} \tag{A6}$$

In the case of the process $\pi^0\eta \to \pi^0\eta$, the SRA amplitude is given by

$$\begin{aligned}T^{\mathrm{SRA}}(s,t,u) = &-\frac{1}{3f_\pi^2}m_\pi^2 + \frac{2(-2c_m m_\pi^2 + c_d(m_\eta^2 + m_\pi^2 - s))^2}{3f_\pi^4(s - m_{S_8}^2)} \\ &+ \frac{4(2(-\tilde{c}_d + \tilde{c}_m)m_\pi^2 + \tilde{c}_d t)(-6\tilde{c}_d m_\eta^2 + 8\tilde{c}_m m_K^2 - 2\tilde{c}_m m_\pi^2 + 3\tilde{c}_d t)}{3f_\pi^4(t - m_{S_0}^2)} \\ &- \frac{2(2(-c_d + c_m)m_\pi^2 + c_d t)(2c_m(8m_K^2 - 5m_\pi^2) + 3c_d(-2m_\eta^2 + t))}{9f_\pi^4(t - m_{S_8}^2)} \\ &+ \frac{2(-2c_m m_\pi^2 + c_d(m_\eta^2 + m_\pi^2 - u))^2}{3f_\pi^4(u - m_{S_8}^2)} - \frac{8d_m^2 m_\pi^4}{3f_\pi^4(m_\pi^2 - m_{P_8}^2)} + \frac{16d_m^2 m_\pi^2(m_\pi^2 - 4m_K^2)}{9f_\pi^4(m_\eta^2 - m_{P_8}^2)} \\ &+ \frac{64\tilde{d}_m^2 m_\pi^2(m_K^2 - m_\pi^2)}{3f_\pi^4(m_\eta^2 - m_{P_0}^2)} + \frac{32c_d c_m m_\pi^2(m_K^2 + m_\pi^2)}{9f_\pi^4 m_{S_8}^2}. \end{aligned} \tag{A7}$$

Finally, for the channel $\eta\eta \to \eta\eta$ it reads

$$\begin{aligned}T^{\mathrm{SRA}}(s,t,u) = &\frac{7m_\pi^2 - 16m_K^2}{9f_\pi^2} + \frac{4(6\tilde{c}_t m_\eta^2 - 8\tilde{c}_m m_K^2 + 2\tilde{c}_m m_\pi^2 - 3\tilde{c}_d s)^2}{9f_\pi^4(s - m_{S_0}^2)} + \frac{2(6c_d m_\eta^2 - 16c_m m_K^2 + 10c_m m_\pi^2 - 3c_d s)^2}{27f_\pi^4(s - m_{S_8}^2)} \\ &+ \frac{4(6\tilde{c}_t m_\eta^2 - 8\tilde{c}_m m_K^2 + 2\tilde{c}_m m_\pi^2 - 3\tilde{c}_d t)^2}{9f_\pi^4(t - m_{S_0}^2)} + \frac{2(6c_d m_\eta^2 - 16c_m m_K^2 + 10c_m m_\pi^2 - 3c_d t)^2}{27f_\pi^4(t - m_{S_8}^2)} \\ &+ \frac{4(6\tilde{c}_t m_\eta^2 - 8\tilde{c}_m m_K^2 + 2\tilde{c}_m m_\pi^2 - 3\tilde{c}_d u)^2}{9f_\pi^4(u - m_{S_0}^2)} + \frac{2(6c_d m_\eta^2 - 16c_m m_K^2 + 10c_m m_\pi^2 - 3c_d u)^2}{27f_\pi^4(u - m_{S_8}^2)} \\ &- \frac{128\tilde{d}_m^2(5m_\pi^4 + 8m_K^4 - 13m_K^2 m_\pi^2)}{9f_\pi^4(m_\eta^2 - m_{P_0}^2)} - \frac{32d_m^2(64m_K^4 - 44m_K^2 m_\pi^2 + 7m_\pi^4)}{27f_\pi^4(m_\eta^2 - m_{P_8}^2)} + \frac{128d_m^2 m_K^4}{9f_\pi^4(m_K^2 - m_{P_8}^2)} \\ &- \frac{56d_m^2 m_\pi^4}{9f_\pi^4(m_\pi^2 - m_{P_8}^2)} + \frac{64c_m(m_K^2 - m_\pi^2)(10c_d m_K^2 - 6c_m m_K^2 - 7c_d m_\pi^2 + 6c_m m_\pi^2)}{27f_\pi^4 m_{S_8}^2}. \end{aligned} \tag{A8}$$

For the sake of completeness, we have checked, for each of the considered processes, that the above formulas are equivalent to the $\mathcal{O}(p^4)$ contributions proportional to the LECs L_i of Ref. [52], when the following relations hold:

$$\begin{aligned}&L_1 = \frac{G_V^2}{8m_V^2} - \frac{c_d^2}{6m_{S_8}^2} + \frac{\tilde{c}_d^2}{2m_{S_0}^2}, \qquad L_2 = \frac{G_V^2}{4m_V^2}, \qquad L_3 = \frac{-3G_V^2}{4m_V^2} + \frac{c_d^2}{2m_{S_8}^2}, \\ &L_4 = -\frac{c_d c_m}{3m_{S_8}^2} + \frac{\tilde{c}_d\tilde{c}_m}{m_{S_0}^2}, \qquad L_5 = \frac{c_d c_m}{m_{S_8}^2}, \qquad L_6 = -\frac{c_m^2}{6m_{S_8}^2} + \frac{\tilde{c}_m^2}{2m_{S_0}^2}, \qquad L_8 = -3L_6, \\ &L_7 = \frac{d_m^2}{6m_{P_8}^2} - \frac{\tilde{d}_m^2}{2m_{P_0}^2}, \qquad L_8 = \frac{c_m^2}{2m_{S_8}^2} - \frac{d_m^2}{2m_{P_8}^2}. \end{aligned} \tag{A9}$$

[1] P. Langacker and H. Pagels, Phys. Rev. D **8**, 4595 (1973).
[2] A. Pich, Rep. Prog. Phys. **58**, 563 (1995).
[3] G. Ecker, Prog. Part. Nucl. Phys. **35**, 1 (1995).
[4] G. 't Hooft, Nucl. Phys. **B72**, 461 (1974).
[5] E. Witten, Nucl. Phys. **B160**, 57 (1979).
[6] B. Lucini and M. Panero, Prog. Part. Nucl. Phys. **75**, 1 (2014).
[7] S. Weinberg, Physica A (Amsterdam) **A96**, 327 (1979).
[8] T. Appelquist and C. W. Bernard, Phys. Rev. D **23**, 425 (1981).

[9] J. Gasser and H. Leutwyler, Ann. Phys. (N.Y.) **158**, 142 (1984).
[10] J. Gasser and H. Leutwyler, Nucl. Phys. **B250**, 465 (1985).
[11] G. Ecker, J. Gasser, A. Pich, and E. de Rafael, Nucl. Phys. **B321**, 311 (1989).
[12] G. Ecker, J. Gasser, H. Leutwyler, A. Pich, and E. de Rafael, Phys. Lett. B **223**, 425 (1989).
[13] V. Cirigliano, G. Ecker, M. Eidemüller, R. Kaiser, A. Pich, and J. Portolés, Nucl. Phys. **B753**, 139 (2006).
[14] A. Pich, arXiv:hep-ph/0205030.
[15] K. Kampf and B. Moussallam, Eur. Phys. J. **C47**, 723 (2006).
[16] J. Nieves, A. Pich, and E. Ruiz Arriola, Phys. Rev. D **84**, 096002 (2011).
[17] J. Nieves and E. Ruiz Arriola, Nucl. Phys. **A679**, 57 (2000).
[18] P. Masjuan, E. Ruiz Arriola, and W. Broniowski, Phys. Rev. D **87**, 014005 (2013).
[19] R. Tarrach, Z. Phys. **C2**, 221 (1979).
[20] A. Bramon and E. Masso, Phys. Lett. **104B**, 311 (1981).
[21] D. Espriu, E. de Rafael, and J. Taron, Nucl. Phys. **B345**, 22 (1990).
[22] E. Ruiz Arriola and W. Broniowski, Phys. Rev. D **67**, 074021 (2003).
[23] E. Megias, E. Ruiz Arriola, L. Salcedo, and W. Broniowski, Phys. Rev. D **70**, 034031 (2004).
[24] J. Nieves and E. R. Arriola, Phys. Rev. D **80**, 045023 (2009).
[25] J. Nieves and E. Ruiz Arriola, Phys. Lett. B **679**, 449 (2009).
[26] J. Bijnens, E. Gamiz, E. Lipartia, and J. Prades, J. High Energy Phys. 04 (2003) 055.
[27] P. Roig and J. J. Sanz-Cillero, Phys. Lett. B **733**, 158 (2014).
[28] J. R. Pelaez, Phys. Rev. Lett. **92**, 102001 (2004).
[29] J. Ruiz de Elvira, J. Pelaez, M. Pennington, and D. Wilson, Phys. Rev. D **84**, 096006 (2011).
[30] Z.-H. Guo and J. Oller, Phys. Rev. D **84**, 034005 (2011).
[31] Z.-H. Guo, J. Oller, and J. Ruiz de Elvira, Phys. Rev. D **86**, 054006 (2012).
[32] Z.-H. Guo, J. Oller, and J. Ruiz de Elvira, Phys. Lett. B **712**, 407 (2012).
[33] T. Cohen, F. J. Llanes-Estrada, J. Pelaez, and J. R. de Elvira, Phys. Rev. D **90**, 036003 (2014).
[34] G. Bali, F. Bursa, L. Castagnini, S. Collins, L. Del Debbio, B. Lucini, and M. Panero, J. High Energy Phys. 06 (2013) 071.
[35] G. S. Bali, L. Castagnini, B. Lucini, and M. Panero, *Proc. Sci.*, LATTICE2013 (2013) 100.
[36] O. Cata and S. Peris, Phys. Rev. D **65**, 056014 (2002).
[37] I. Rosell, J. J. Sanz-Cillero, and A. Pich, J. High Energy Phys. 08 (2004) 042.
[38] I. Rosell, P. Ruiz-Femenia, and J. Portoles, J. High Energy Phys. 12 (2005) 020.
[39] I. Rosell, J. J. Sanz-Cillero, and A. Pich, J. High Energy Phys. 01 (2007) 039.
[40] A. Pich, I. Rosell, and J. J. Sanz-Cillero, J. High Energy Phys. 07 (2008) 014.
[41] A. Pich, I. Rosell, and J. J. Sanz-Cillero, J. High Energy Phys. 02 (2011) 109.
[42] J. J. Sanz-Cillero and J. Trnka, Phys. Rev. D **81**, 056005 (2010).
[43] J. Beringer *et al.* (Particle Data Group), Phys. Rev. D **86**, 010001 (2012).
[44] E. Ruiz Arriola and W. Broniowski, arXiv:1110.2863.
[45] P. Masjuan, E. Ruiz Arriola, and W. Broniowski, Phys. Rev. D **85**, 094006 (2012).
[46] S. Peris and E. de Rafael, Phys. Lett. B **348**, 539 (1995).
[47] G. Ecker, Acta Phys. Pol. B **38**, 2753 (2007).
[48] J. Bijnens and I. Jemos, Nucl. Phys. **B854**, 631 (2012).
[49] J. Bijnens and G. Ecker, arXiv:1405.6488.
[50] M. Gonzalez-Alonso, A. Pich, and J. Prades, Phys. Rev. D **78**, 116012 (2008).
[51] P. A. Boyle, L. Del Debbio, N. Garron, R. J. Hudspith, E. Kerrane, K. Maltman, and J. M. Zanotti, Phys. Rev. D **89**, 094510 (2014).
[52] A. Gomez Nicola and J. Pelaez, Phys. Rev. D **65**, 054009 (2002).
[53] J. Nieves and E. Ruiz Arriola, Phys. Lett. B **455**, 30 (1999).
[54] J. Nieves and E. Ruiz Arriola, Phys. Rev. D **64**, 116008 (2001).
[55] R. Garcia-Martin, R. Kaminski, J. Pelaez, J. Ruiz de Elvira, and F. Yndurain, Phys. Rev. D **83**, 074004 (2011).
[56] J. Batley *et al.* (NA48-2 Collaboration), Eur. Phys. J. C **70**, 635 (2010).
[57] P. Buettiker, S. Descotes-Genon, and B. Moussallam, Eur. Phys. J. C **33**, 409 (2004).
[58] G. P. Lepage, B. Clark, C. T. H. Davies, K. Hornbostel, P. B. Mackenzie, C. Morningstar, and H. Trottier, Nucl. Phys. B, Proc. Suppl. **106**, 12 (2002).
[59] C. Morningstar, Nucl. Phys. B, Proc. Suppl. **109A**, 185 (2002).
[60] M. R. Schindler and D. R. Phillips, Ann. Phys. (Amsterdam) **324**, 682 (2009).
[61] M. Jamin, J. A. Oller, and A. Pich, Nucl. Phys. **B587**, 331 (2000).
[62] R. Garcia-Martin, R. Kaminski, J. Pelaez, and J. Ruiz de Elvira, Phys. Rev. Lett. **107**, 072001 (2011).
[63] S. Descotes-Genon and B. Moussallam, Eur. Phys. J. C **48**, 553 (2006).
[64] I. Caprini, G. Colangelo, and H. Leutwyler, Phys. Rev. Lett. **96**, 132001 (2006).
[65] M. Albaladejo and J. Oller, Phys. Rev. Lett. **101**, 252002 (2008).
[66] L. Geng and E. Oset, Phys. Rev. D **79**, 074009 (2009).
[67] C. Garcia-Recio, L. Geng, J. Nieves, and L. Salcedo, Phys. Rev. D **83**, 016007 (2011).
[68] C. García-Recio, L. S. Geng, J. Nieves, L. L. Salcedo, E. Wang, and J.-J. Xie, Phys. Rev. D **87**, 096006 (2013).